Plant Molecular Biology (2024) 114:55
https://doi.org/10.1007/s11103-024-01458-5

Transcriptome analysis and functional validation reveal the novel role of *LhCYCL* in axillary bud development in hybrid *Liriodendron*

Shaoying Wen[1,2] · Qinghua Hu[1,2] · Jing Wang[1,2] · Huogen Li[1,2]

Received: 27 September 2023 / Accepted: 25 April 2024 / Published online: 10 May 2024
© The Author(s), under exclusive licence to Springer Nature B.V. 2024

Abstract

Shoot branching significantly influences yield and timber quality in woody plants, with hybrid *Liriodendron* being particularly valuable due to its rapid growth. However, understanding of the mechanisms governing shoot branching in hybrid *Liriodendron* remains limited. In this study, we systematically examined axillary bud development using morphological and anatomical approaches and selected four distinct developmental stages for an extensive transcriptome analysis. A total of 9,449 differentially expressed genes have been identified, many of which are involved in plant hormone signal transduction pathways. Additionally, we identified several transcription factors downregulated during early axillary bud development, including a noteworthy gene annotated as *CYC-like* from the TCP TF family, which emerged as a strong candidate for modulating axillary bud development. Quantitative real-time polymerase chain reaction results confirmed the highest expression levels of *LhCYCL* in hybrid *Liriodendron* axillary buds, while histochemical β-glucuronidase staining suggested its potential role in *Arabidopsis thaliana* leaf axil development. Ectopic expression of *LhCYCL* in *A. thaliana* led to an increase of branches and a decrease of plant height, accompanied by altered expression of genes involved in the plant hormone signaling pathways. This indicates the involvement of *LhCYCL* in regulating shoot branching through plant hormone signaling pathways. In summary, our results emphasize the pivotal role played by *LhCYCL* in shoot branching, offering insights into the function of the *CYC-like* gene and establishing a robust foundation for further investigations into the molecular mechanisms governing axillary bud development in hybrid *Liriodendron*.

Key message

This study systematically observed the axillary bud development in hybrid *Liriodendron* and found that *LhCYCL* promotes shoot branching by precisely regulating the expression of plant hormone signaling pathway genes.

Keywords Hybrid *Liriodendron* · Axillary bud · *LhCYCL* · Shoot branching

Introduction

Shoot branching is an important trait that shapes plant architecture, a result of the intricate spatiotemporal regulation governing axillary bud development (Rameau et al. 2015). The process begins with the formation of axillary buds in the leaf axils, followed by their subsequent outgrowth into branches (Domagalska and Leyser 2011). Notably, axillary bud outgrowth is an exceptionally adaptable phenomenon (Domagalska and Leyser 2011), finely orchestrated by a complex interplay of both internal and external signals (Luo et al. 2021).

Plant hormones, such as auxin, cytokinin (CK), gibberellin (GA), abscisic acid (ABA), brassinosteroid (BR), and strigolactone (SL), have been identified as key players in the regulation of axillary bud outgrowth (Janssen et al. 2014; Nguyen and Emery 2017; Katyayini et al. 2020). Numerous studies have demonstrated that the application of exogenous CK or the controlled manipulation of endogenous CK levels not only promotes axillary bud outgrowth in herbaceous plants but also in perennial woody plants such as *Populus*

✉ Huogen Li
hgli@njfu.edu.cn

[1] State Key Laboratory of Tree Genetics and Breeding, Nanjing Forestry University, Nanjing 210037, Jiangsu, China

[2] Co-Innovation Center for Sustainable Forestry in Southern China, Nanjing Forestry University, Nanjing 210037, Jiangsu, China

trichocarpa, *Jatropha curcas*, *Malus domestica* and *Prunus persica* (Faiss et al. 1997; Chatfield et al. 2000; Cline et al. 2006; Ni et al. 2015; Waldie and Leyser 2018; Qiu et al. 2019; Tan et al. 2019; Li et al. 2021). Notably, components involved in CK biosynthesis and signal transduction, such as iso pentenyl transferase (IPT) and arabidopsis response regulator (ARR), play significant roles in this process. For instance, mutants like *ipt3*,*5*,*7* and *arr3*,*4*,*5*,*6*,*7*,*15*, when compared to WT *Arabidopsis thaliana*, exhibit reduced rosette branching (Müller et al. 2015). Additionally, studies have shown that manipulating the expression of *IPT* genes can have a profound impact on axillary bud outgrowth. For instance, the defective axillary meristem initiation observed in the *rax1-3* mutant can be rescued through the expression of *IPT8* (Wang et al. 2014). Furthermore, researchers have noted that upon decapitation or stem girdling treatments, increased expression levels of *IPT1* and *IPT2* are correlated with enhanced bud outgrowth (Ferguson and Beveridge 2009). Likewise, the expression levels of *PpIPT1*, *PpIPT3*, and *PpIPT5a* in peach stem nodes substantially rise following decapitation, thereby promoting axillary bud outgrowth (Li et al. 2018). Ectopic expression of *M. domestica* type-A RRs *RR9* increased the number of lateral branches in tomatoes, revealing that *MdRR9* plays a positive role in regulating shoot branching (Zhao et al. 2023). Moreover, type-B ARRs, known as CK response genes, are capable of directly binding to the *WUSCHEL* (*WUS*) promoter, activating its expression and thereby stimulating axillary meristem initiation (Wang et al. 2017).

CK functions as a secondary messenger in the modulation of axillary bud activity in response to auxin signals. Research has revealed that auxin regulates CK biosynthesis by suppressing the expression of *IPT* genes (Tanaka et al. 2006). Furthermore, CK plays a role in mediating auxin transport by affecting the levels of PIN-formed 3 (PIN3), PIN4, and PIN7 proteins in inflorescence stems (Waldie and Leyser 2018). In the case of rice, SLs reduce CK levels by influencing the expression of *CYTOKININ OXIDASE/DEHYDROGENASE 9* (*CKX9*) (Duan et al. 2019). Notably, SL-deficient mutants of peas and rice exhibit higher CK levels compared to WT plants (Young et al. 2014; Duan et al. 2019). Additionally, in *Pisum sativum*, CK regulates the expression of the negative regulator of SL signaling, *SUPPRESSOR OF MAX2-LIKE 7* (*SMXL7*) (Kerr et al. 2021). It is worth noting that CK exerts antagonistic effects on auxin and SLs when it comes to regulating axillary bud growth.

In recent years, numerous studies have highlighted the pivotal role of sugar in promoting bud outgrowth, emphasizing its significance as a key player in this process (Rabot et al. 2012; Barbier et al. 2015; Fichtner et al. 2017). Sugar can intricately interact with hormone pathways to effectively regulate shoot branching (Barbier et al. 2019). For instance, sucrose has been shown to accelerate auxin synthesis in a concentration-dependent manner while also inducing the export of auxin from buds (Barbier et al. 2015). Furthermore, sugars contribute to bud outgrowth by facilitating the accumulation of CK (Salam et al. 2021). These findings collectively underscore the intricate and multifaceted nature of the regulatory network governing axillary bud outgrowth (Luo et al. 2021). Within this intricate regulatory network, transcription factors (TFs) play a crucial role. Various TF families, including MADS, NAC, HB-KNOX, MYB, WOX, GRAS, bHLH, AP2/ERF, TCP, LOB, WRKY, HD-ZIP, and SBP, have been reported to be involved in the regulation of shoot branching (Zhang et al. 2022). Notably, CK can modulate the expression of certain TCP genes. For instance, elevated CK levels in axillary buds inhibit the expression of *BRC1*, thereby promoting axillary bud activation (Braun et al. 2012). In the context of rice, CKs have been demonstrated to reduce the transcriptional level of *OsTB1* in a dose-dependent manner (Minakuchi et al. 2010). Additionally, Steiner *et al.* proposed that CK enhances the activities of *AtTCP14/15,* with *AtTCP14/15* augmenting the plant sensitivity to CK (Steiner et al. 2012).

The TCP family members can be classified into three distinct clades: PCF, CIN, and CYC/TB1 (Zhou et al. 2022). Notably, ectopic expression of *AtTCP14* and *AtTCP15* (belonging to the PCF clade TCPs) has been found to increase the number of branches in tomato plants (Steiner et al. 2012). In contrast, certain genes within the CYC/TB1 clade have emerged as key regulators in the development of axillary meristems, which can lead to the formation of either flowers or lateral branches (Martin-Trillo and Cubas 2010). Zhao *et al.* demonstrated that genes from the *Broussonetia papyrifera* CYC/TB1 clade, specifically *BpTCP8*, *BpTCP14*, and *BpTCP19*, play roles in inhibiting the outgrowth of primary branches (Zhao et al. 2020). Furthermore, CYC/TB1 genes have undergone several duplications and diversifications at the base of core eudicots, giving rise to the CYC1, CYC2, and CYC3 clades (Howarth and Donoghue 2006; Citerne et al. 2013). Within these clades, the CYC1 clade gene *TCP18/BRC1* in dicotyledons and its closest homolog, *TB1*, in monocots, are central hub genes deeply involved in the regulation of shoot branching (Wang et al. 2019). Phylogenetic analysis has revealed that the *Gossypium hirsutum TCP62* gene belongs to the TB1 subfamily, and *GhTCP62* has been shown to exert a negative regulatory effect on shoot branching in *A. thaliana* (Liu et al. 2021). Similarly, the expression analysis of sunflower *TCP1* (a homologous gene of *AtBRC1*) has indicated a high enrichment in buds, and overexpression of *HaTCP1* in *A. thaliana* significantly reduced the number of stem and rosette branches (Wu et al. 2023). In addition, the CYC2 clade gene *AtTCP1* plays a role in mediating the BR biosynthesis pathway by positively regulating the transcription of the BR biosynthesis gene *DWARF4* (*DWF4*) (An et al. 2011). Overexpression of

SlTCP26, a gene closely related to *AtTCP1*, has been found to stimulate the development of lateral branches in tomato plants (Wei et al. 2021). Moreover, heterologous expression of the *M. domestica* CYC3 clade gene *MdTCP12* has led to a reduction in the number of rosette branches in *A. thaliana* (Li et al. 2021). Compared to the wild-type plants, the *Populus BRC2-1* mutants exhibited significantly increased branch numbers (Muhr et al. 2018). In summary, distinct *TCP* genes perform specific functions in the regulation of lateral branch development.

The hybrid *Liriodendron*, a deciduous tree belonging to the Magnoliaceae family, is the result of a cross between *Liriodendron chinense* (Hemsl.) Sarg. as the female parent and *Liriodendron tulipifera* Linn. as the male parent. This hybrid species is renowned for its rapid growth and superior wood quality, rendering it an exceptional choice for construction and furniture manufacturing (Xiang and Wang 2012). However, a notable challenge with the hybrid *Liriodendron* is its tendency to develop multiple branches along the main stem, which significantly impacts both timber yield and quality. Despite its many advantages, the precise mechanisms governing the growth and development of axillary buds in hybrid *Liriodendron* remain poorly understood. As a result, efforts to genetically enhance its branching characteristics have been hindered by this lack of knowledge.

In this study, we conducted a comprehensive evaluation of the axillary bud development process in hybrid *Liriodendron*. We meticulously selected four crucial developmental stages of axillary buds for transcriptome sequencing analysis. Throughout the course of axillary bud development, we identified numerous DEGs, among which the *LhCYCL* gene emerged as a promising candidate gene associated with axillary bud development. Subsequent experiments involving the ectopic expression of *LhCYCL* in *A. thaliana* resulted in a significant increase in the number of branches, suggesting that *LhCYCL* likely plays a pivotal role in the development of axillary buds in hybrid *Liriodendron*. This research not only unveils novel functions of the *LhCYCL* gene but also makes a valuable contribution to our understanding of the molecular mechanisms governing axillary bud development in hybrid *Liriodendron*.

Materials and methods

Plant materials and growth conditions

The hybrid *Liriodendron* 334 is an artificial hybrid clone obtained from *Liriodendron tulipifera* Linn. (Missouri provenance) as the female parent and *Liriodendron chinense* (Hemsl.) Sarg. (Lushan provenance) as the male parent. Compared to its parent trees, hybrid clone 334 has more branches. In June 2020, we collected healthy semi-lignified branches from a nine-year-old hybrid *Liriodendron* clone 334. These branches were obtained from the experimental station of Nanjing Forestry University, situated in Baima town, Lishui County, Jiangsu province (coordinates: 31° 61′ N, 119° 19′ E). The collected cuttings were then planted in the greenhouse at the Baima base and received regular water and fertilizer management. By June 2022, we selected some cutting plantlets that displayed consistent growth for further experiments. Furthermore, we obtained samples from various parts of the hybrid *Liriodendron*, including the root, stem, leaf, flower, apical bud, sepal, petal, stamen, and pistil. These samples were sourced from hybrid *Liriodendron* plants cultivated in the forestry farm of Nanjing Forestry University, specifically in Xiashu, Jurong, Jiangsu province (coordinates: 32° 12′ N, 119° 23′ E). Immediately upon collection, these samples were flash-frozen in liquid nitrogen and subsequently stored in a −80 ℃ freezer until RNA extraction.

For our experiments involving *A. thaliana*, we used wild-type plants of the *Columbia-0* (*Col-0*) ecotype. *A. thaliana* seeds underwent surface sterilization with 75% alcohol, repeated three times, and were uniformly sown on Murashige and Skoog (MS) medium containing 1% (w/v) sucrose, 0.443% (w/v) MS powder, and 0.8% (w/v) agar (pH 5.8). After vernalization for 2 days at 4 °C, 7-day-old seedlings were transplanted into pots filled with peat soil. *Nicotiana benthamiana* (*Ben*) seeds were germinated by directly sowing them over the soil surface. Subsequently, both *A. thaliana* and *N. benthamiana* were cultivated in an incubator maintained at 22 °C with 60% relative humidity, operating under a 16 h light/8 h dark photoperiod.

Morphological observation and histological studies

Four statuses of axillary bud development were defined based on the growth traits of hybrid *Liriodendron* axillary buds: P1, the axillary bud reached 0.05–0.1 cm in length; P2, the axillary bud reached 0.1–0.2 cm in length; P3, the axillary bud reached 0.2–0.3 cm in length; P4, the axillary bud reached 0.4–0.5 cm in length. The axillary buds from different developmental periods mentioned above were collected individually and immediately fixed in the FAA solution (10% (v/v) formaldehyde, 5% (v/v) acetic acid, 50% (v/v) ethanol) at 4 °C for 3 days. Afterward, they were dehydrated and embedded in paraffin. Subsequently, these samples were longitudinally sliced into 8 μm thick sections using a Leica RM2245 microtome. The sections were stained with Safranine and Fast Green before being photographed with a microscope.

Plant sampling

The axillary buds of the hybrid *Liriodendron* were sampled at four distinct developmental stages, denoted as P1, P2, P3, and P4. These samples were promptly immersed in liquid nitrogen and stored in a −80 °C ultra-low temperature freezer until RNA extraction. In order to ensure an adequate number of samples for each developmental stage, we combined 10–15 axillary buds to form a single replicate, and each stage was represented by three biological replicates.

RNA extraction, library construction, and sequencing

The samples' total RNA was extracted utilizing TRIzol® Reagent (Invitrogen), following the manufacturer's instructions, and any genomic DNA present was removed using DNase I (Takara). To assess both the quality and quantity of the extracted RNA, we employed the 2100 Bioanalyzer (Agilent) and ND-2000 (NanoDrop Technologies), respectively. For the subsequent steps, 1 μg of high-quality RNA was employed in the construction of the RNA-seq transcriptome library using the Illumina TruSeqTM RNA sample preparation kit (San Diego, CA, USA), following the manufacturer's provided protocols. These libraries were subjected to sequencing on the Illumina NovaSeq 6000 sequencing platform, resulting in the generation of 150 bp paired-end reads (performed by Shanghai BIOZERON Co., Ltd).

Transcriptome analysis

The raw paired-end reads underwent trimming and filtering using Trimmomatic 0.36 (http://www.usadellab.org/cms/uploads/supplementary/Trimmomatic) (Bolger et al. 2014). Subsequently, the clean reads were aligned to the *L. chinense* reference genome (Chen et al. 2019) using HISAT2 (https://ccb.jhu.edu/software/hisat2/index.shtml) (Kim et al. 2019). Gene expression levels were quantified as transcripts per million (TPM) (Wagner et al. 2012). To assess the biological variability among the samples, Pearson correlation coefficients were computed, and the results were visually represented in a heatmap. Differential expression analysis was carried out using the R statistical package edgeR, with the following criteria: |log2 Fold Change (FC)|≥ 1 and a false discovery rate (FDR) ≤ 0.05. A Venn diagram was utilized to illustrate the number of specific and shared DEGs across different developmental stages. To elucidate the functions of these DEGs, GO functional enrichment and KEGG pathway analyses were conducted using Goatools (https://github.com/tanghaibao/Goatools) and KOBAS (http://kobas.cbi.pku.edu.cn/home.do). Significantly enriched GO terms and metabolic pathways were identified with a Bonferroni-corrected P-value < 0.05 and can be visualized online at https://www.chiplot.online/. Moreover, DEGs were further subjected to cluster analysis based on standardized TPM values using the Mfuzz R package with the fuzzy c-means algorithm. And the results were visualized through the online tool available at https://www.bioladder.cn/web/#/chart/62. The PlantTFDB (http://planttfdb.gao-lab.org/index.php) was employed to predict the TFs among the DEGs, providing insight into their regulatory roles.

Quantitative real-time PCR

To validate the reliability of the RNA-seq data, we selected nine DEGs—*WUS*, *MYB105*, *CUC2*, *RAX2*, *LFY*, *ERF53*, *HB40*, and *DRNL*, known for their significant roles in axillary bud development in other species (Zhang et al. 2022). Gene-specific primers for qRT-PCR were designed using Primer3 and are provided in Table S1. Initially, total RNA was reverse transcribed into first-strand cDNA using the Evo M-MLV Premix for qPCR kit from Accurate Biotechnology (Hunan) Co., Ltd. Subsequently, qRT-PCR reactions were conducted on the ABI StepOne cycler (Applied Biosystems, USA) employing the SYBR®Green Premix Pro Taq HS qPCR kit from Accurate Biotechnology (Hunan) Co., Ltd. Each qRT-PCR experiment was replicated three times. To normalize the gene expression values, *Actin97* served as the reference gene (Tu et al. 2019). The relative expression levels of the selected DEGs were calculated using the $2^{-\Delta\Delta CT}$ method (Livak and Schmittgen 2001). Furthermore, we applied the same method to assess the expression level of *LhCYCL* in various tissues of hybrid *Liriodendron* and to examine the expression of specific genes in both WT and transgenic *A. thaliana* plants.

Cloning of *LhCYCL* and *LhCYCL* promoter

From the axillary bud transcriptome of the hybrid *Liriodendron*, we identified a gene labeled as *CYC-like*. To acquire reference sequences for both the coding sequence (CDS) of *LhCYCL* and its promoter, we relied on the *L. chinense* genome (Chen et al. 2019). Total RNA was extracted from axillary buds using the RNAprep Pure Plant Kit from Tiangen, Beijing, China, while genomic DNA was obtained from the leaves of hybrid *Liriodendron* using the Trelief® Hi-Pure Plant Genomic DNA Kit from Tsingke, Beijing, China. Subsequently, the first-strand cDNA for the axillary bud was synthesized following the previously described method. We employed the ApexHF HS DNA Polymerase FS Master Mix from Accurate Biotechnology (Hunan) Co., Ltd, along with specific primers, to amplify the CDS of *LhCYCL* and the 2 Kb upstream promoter regions, using both the cDNA and genomic DNA as templates. The resulting PCR products were purified, cloned into a *pEASY*-blunt vector from

TransGen, Beijing, China, and then introduced into *E. coli* for sequencing.

Bioinformatic analyses of *LhCYCL*

The sequences of both *LhCYCL* CDS and *LhCYCLpro* were obtained upon successful sequencing validation. We employed WoLF PSORT (https://wolfpsort.hgc.jp/) for predicting the subcellular localization of LhCYCL. Amino acid sequences of CYCL from various species were retrieved from GenBank (http://www.ncbi.nlm.nih.gov/genbank). Multiple sequence alignment of LhCYCL and other CYC/TB1 proteins was conducted using ClustalW (https://www.genome.jp/tools-bin/clustalw). The results were visualized using ESPript 3.0 (http://espript.ibcp.fr/ESPript/cgi-bin/ESPript.cgi). To examine the evolutionary relationships among homologous CYC/TB1 proteins across different species, we constructed a phylogenetic tree using MEGA X with the neighbor-joining method. Additionally, we utilized Plantcare (http://bioinformatics.psb.ugent.be/webtools/plantcare/html/) to analyze the cis-acting elements present in the promoter region of *LhCYCL*.

Plasmid construction

To investigate the subcellular localization and promoter activity of *LhCYCL*, we inserted the CDS sequence and promoter region of *LhCYCL* into two different vectors: pMDC43 and pCAMBIA1301. This resulted in the creation of two distinct plasmids, namely *35S::LhCYCL-GFP* and *LhCYCLpro::GUS*, respectively. Furthermore, for an in-depth exploration of *LhCYCL* functions, we cloned the CDS of *LhCYCL* into the pCAMBIA1300 vector, yielding the recombinant plasmid *35S::LhCYCL-pCAMBIA1300*. Subsequently, the fusion constructs, namely *35S::LhCYCL-GFP*, *LhCYCLpro::GUS*, and *35S::LhCYCL-pCAMBIA1300*, were separately introduced into *Agrobacterium tumefaciens* strain GV3101. The primers used for constructing these vectors are provided in Table S1.

Subcellular localization

In order to investigate the subcellular localization of the LhCYCL protein, we conducted a transient expression experiment in tobacco leaves using the *35S::LhCYCL-GFP* construct, along with control vectors, following the methodology outlined by (Sparkes et al. 2006). The pMDC43 vector was employed as the positive control in this study. Subsequent to 48 h of dark incubation, we visualized the GFP fluorescent signal using a confocal laser scanning microscope (LSM 900, Zeiss, Germany).

Overexpression of *LhCYCL* in *A. thaliana* and phenotype observation

To elucidate the functions of *LhCYCL*, we employed *Agrobacterium tumefaciens* GV3101 harboring the *35S::LhCYCL-pCAMBIA1300* construct to introduce the genetic material into *A. thaliana* via the floral dip method (Clough and Bent 1998). Detection of DNA in the T_1 generation allowed us to identify positive transgenic plants. Subsequently, we selected three independent transgenic lines from the positive *LhCYCL* transgenic group, characterized by higher expression levels, using qRT-PCR. Further analysis involved the generation of T_3-generation homozygous transgenic lines, which were obtained through continuous screening on MS medium supplemented with 30 mg/L Hygromycin B (HygB).

The seeds of both WT and *LhCYCL* transgenic plants were cultivated on MS medium for 7 days before being transplanted into soil. After 30 days of growth under standard conditions, we measured the rosette leaf area of *A. thaliana* plants. Additionally, after 50 days of growth, we conducted phenotypic observations, including measurements of branch number and plant height, on both WT and transgenic plants. These data were collected from ten individual *A. thaliana* plants for both the WT and *LhCYCL* transgenic groups.

Histochemical assay of GUS activity

Similarly, the *LhCYCLpro::GUS* plasmid was introduced into *A. thaliana* following the same procedure as described earlier. Positive transgenic plants from the T_1 generation were identified through PCR analysis. Subsequently, T_2-generation transgenic plants were obtained and subjected to GUS activity analysis after a screening process on HygB-containing medium.

Cytokinin content measurement

Rosette leaves of 0.3 g were collected from 30-day-old WT and *LhCYCL* transgenic *A. thaliana* plants and rapidly frozen in liquid nitrogen. The determination of Zeatin (ZT) content in *A. thaliana* leaves employed Enzyme-Linked Immunosorbent Assay (ELISA) (Huding, Shanghai, China). Three biological replicates were used for each mesurement.

Statistical analysis

SPSS 22.0 software was employed for conducting one-way ANOVA and Duncan's multiple comparisons on all experimental data. The analysis outcomes were illustrated in bar graphs using GraphPad Prism 8. The statistical

representation comprises mean ± standard deviation (SD), with significance indicated by different letters and defined by a P-value threshold of less than 0.05 ($P < 0.05$).

Results

Morphological and anatomical observations of axillary buds

By conducting dynamic observations of axillary bud development in hybrid *Liriodendron*, we initially categorized it into four stages based on bud length: P1 (0.05–0.1 cm), P2 (0.1–0.2 cm), P3 (0.2–0.3 cm), and P4 (0.4–0.5 cm) as shown in Fig. 1A. Longitudinal sections of axillary buds during these developmental stages revealed the presence of a complete apical meristem, displaying a characteristic "tunica-corpus" structure. In the P1 stage, the axillary buds remained in a dormant state, with leaves tightly enveloping the meristem. In P2, there was an increase in the number of leaf blades, and the bases of the outermost two leaf blades began to spread outward. In the P3 stage, the number of leaf blades continued to rise, and the outermost two leaf blades extended further outward, accompanied by a noticeable bulge at the base of these outermost leaf blades. Finally, in the P4 stage, a fully developed axillary meristem was observed at the base of the outermost leaf blades, as illustrated in Fig. 1B. This observation further underscores that the axillary buds possess similar developmental potential to terminal buds.

An overview of the transcriptome data

A total of 12 cDNA libraries were constructed from axillary buds at four distinct developmental stages, each with three biological replicates. Following sequencing, we obtained 12 transcriptomic datasets, and their basic characteristics are summarized in Table S2. Notably, each library contained no fewer than 0.52 billion raw reads. After the application of filtering criteria, we retained over 0.49 billion high-quality reads from each sample. The clean reads exhibited excellent quality, with Q20 values exceeding 97% and Q30 values surpassing 93%. Furthermore, a substantial portion of clean reads, ranging from 81.58 to 86.25%, were successfully mapped to the reference genome. The high degree of correlation among the three biological replicates of each sample was evident from the Pearson correlation coefficient (R^2) values, which approached 1 (Fig. S1A). Additionally, Fig. S1B illustrates the distribution of gene expression levels for each sample, highlighting the relatively consistent gene transcription levels observed among biological duplicates. These findings collectively affirm the high quality of the transcriptome data obtained from hybrid *Liriodendron* axillary buds across various developmental stages.

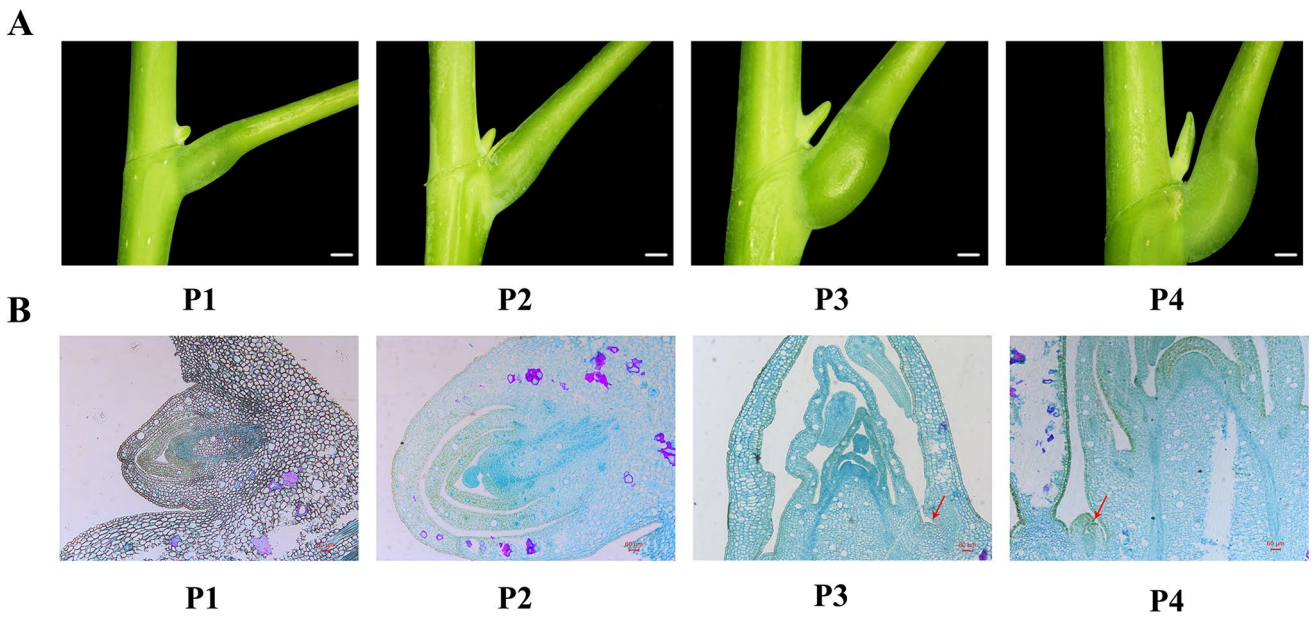

Fig. 1 Morphological and anatomical observations of axillary buds in hybrid *Liriodendron*. **A** Phenotype of axillary bud during different developmental stages in hybrid *Liriodendron*, bars = 0.1 cm. **B** Paraffin sections of axillary bud during different developmental stages in hybrid *Liriodendron*, bars = 60 um. The red arrow indicates the axillary meristem

Identification of DEGs

A large number of DEGs were identified through pairwise comparisons of the RNA-seq data, yielding the following results: P2 VS P1, with 6,721 DEGs (comprising 2,783 upregulated and 3,938 downregulated genes); P3 VS P2, with 1,927 DEGs (comprising 958 upregulated and 969 downregulated genes); and P4 VS P3, with 4,160 DEGs (comprising 1,969 upregulated and 2,191 downregulated genes) (Fig. 2A). Furthermore, a Venn diagram illustrates that 4,190, 506, and 1,730 DEGs were specifically expressed in the P2 VS P1, P3 VS P2, and P4 VS P3 comparison groups, respectively. Notably, there were 336 DEGs commonly identified in all three comparison

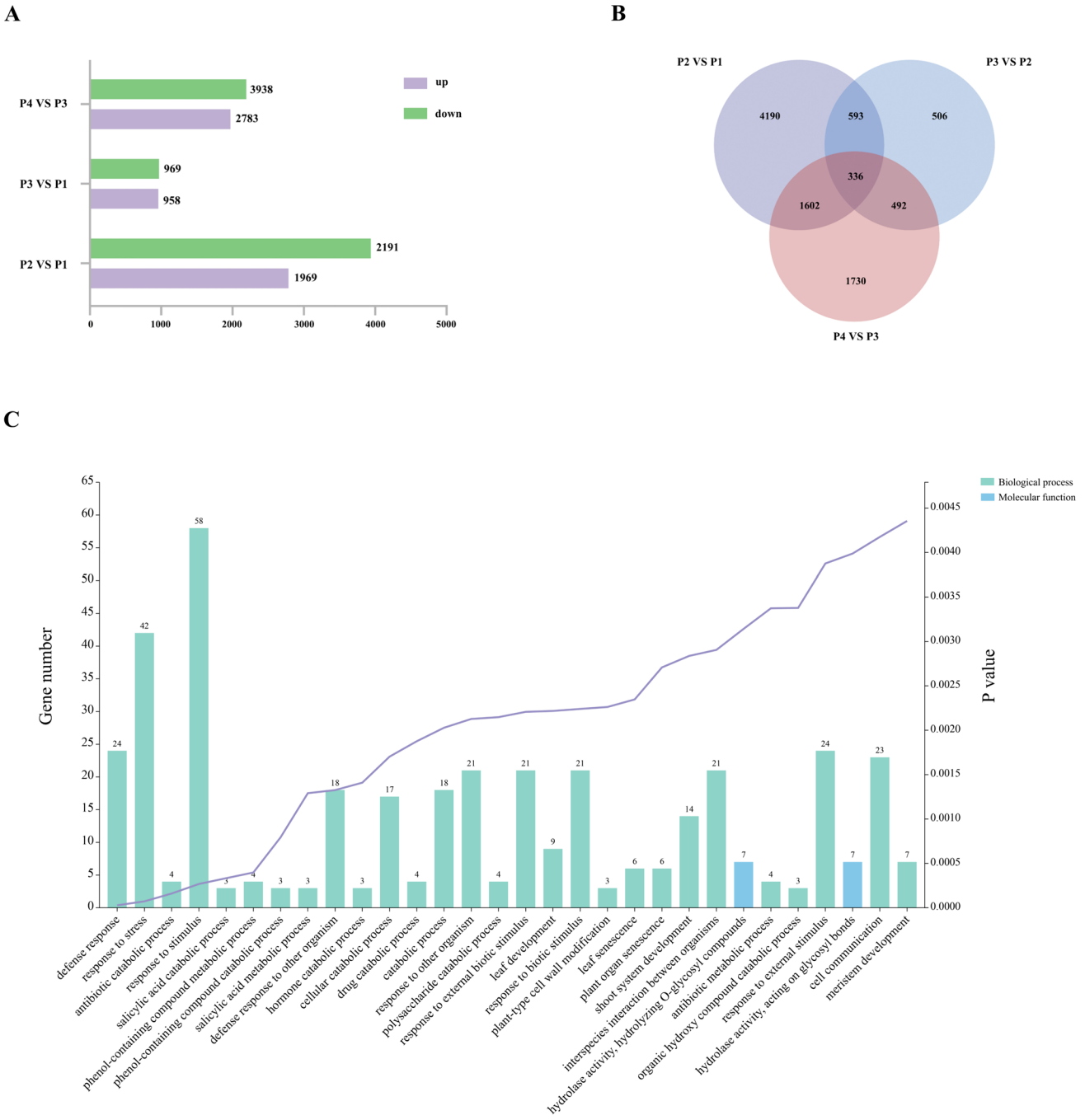

Fig. 2 Overview of the DEGs in pairwise comparisons between four developmental stages of axillary buds. **A** Numbers of up-regulated and down-regulated DEGs identified from the three comparison groups. **B** Venn diagram illustrates the distribution of DEGs in different comparisons. **C** Go terms enrichment analysis of the common DEGs among three comparison groups

groups (as shown in Fig. 2B). To gain insights into the potential functions of these common DEGs, we conducted a GO term enrichment analysis. The results revealed that the majority of these common DEGs were enriched in the biological process category. Within this category, terms such as 'response to stimulus' and 'response to stress' emerged as the two largest groups. Additionally, 'hormone catabolic process', 'shoot system development', and 'meristem development' were prominently enriched terms in the biological process category (Fig. 2C).

KEGG enrichment analysis of DEGs

The DEGs identified in each comparison from the aforementioned analysis underwent further examination via KEGG enrichment analysis. In Fig. 3, we present the top 25 significantly enriched pathways across the two comparison groups. Notably, in the P2 VS P1 comparison, pathways related to axillary bud outgrowth, such as 'Plant hormone signal transduction', 'Starch and sucrose metabolism', and 'Brassinosteroid biosynthesis' displayed significant enrichment. Of particular interest is the consistent enrichment of the 'Plant hormone signal transduction' pathway across all three comparison groups. In the P2 VS

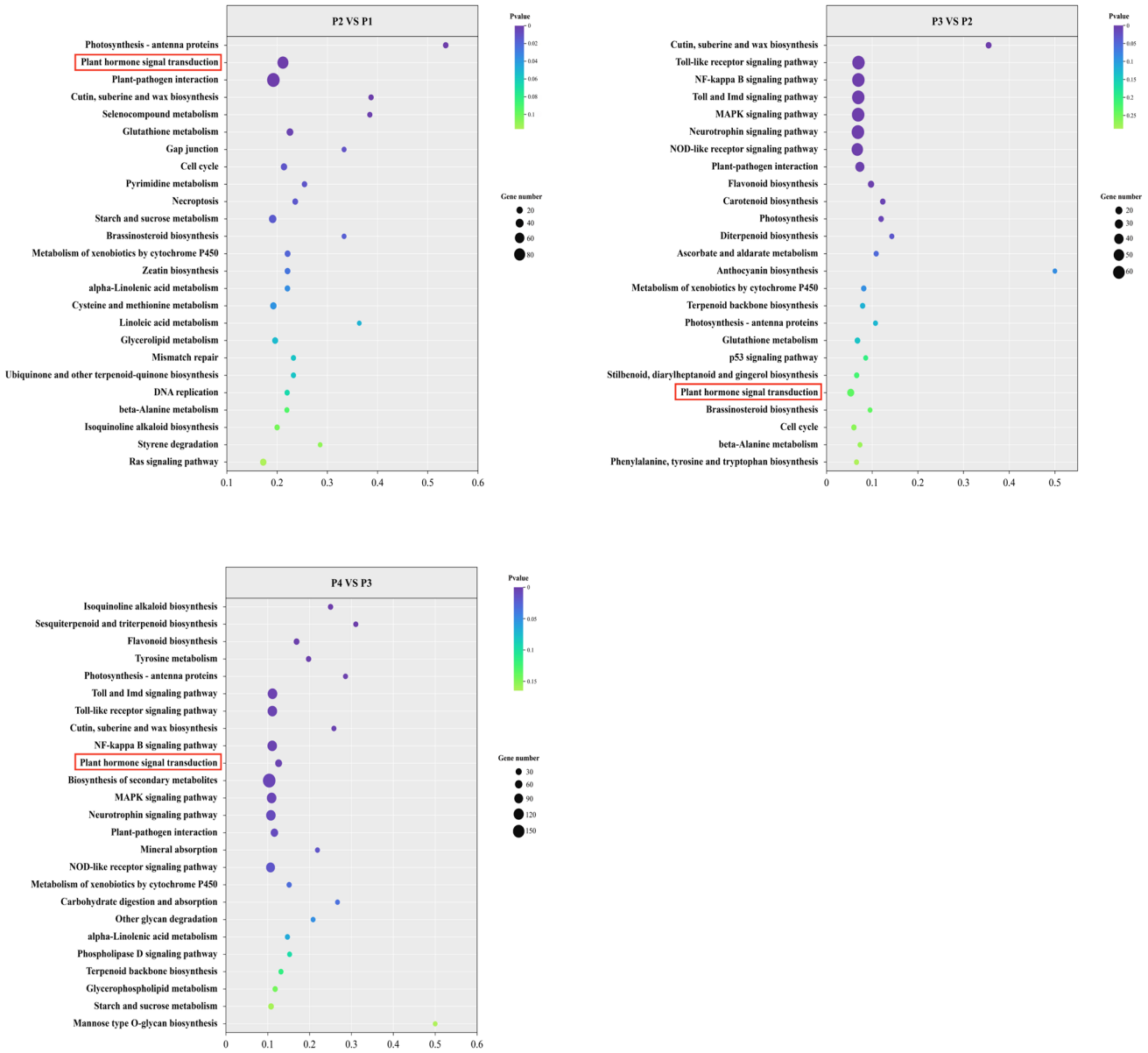

Fig. 3 KEGG enrichment analysis in different comparisons

P1, P3 VS P2, and P4 VS P3 groups, this pathway annotated 84 DEGs (comprising 27 upregulated and 57 downregulated), 21 DEGs (comprising 11 upregulated and 10 downregulated), and 50 DEGs (comprising 25 upregulated and 25 downregulated), respectively. It is noteworthy that the majority of genes enriched in the plant hormone signal transduction pathway exhibited downregulation.

Within the plant hormone signal transduction pathways (Fig. S2), we identified 44, 12, 10, 7, and 17 DEGs involved in Auxin, CK, GA, ABA, and BR signal transduction, respectively. Notably, genes encoding key components such as auxin influx carrier (AUX1), transport inhibitor response 1 (TIR1), auxin/indole-acetic acid inducible (AUX/IAA), Gretchen Hagen 3 (GH3), and small auxin up RNA (SUAR) displayed higher expression levels in the P1 stage. Conversely, two genes encoding the auxin response factor (ARF) exhibited downregulation between P1 and P2. Additionally, one gene encoding the cytokinin receptor protein cytokinin response 1 (CRE1) and three genes encoding the two-component response regulator ARR-A family (A-APP) had their lowest expression levels in P2. Notably, various members of the DELLA family exhibited distinct expression patterns across the four time points, with three DELLAs upregulated and three DELLAs downregulated between P1 and P2. Furthermore, the ABA receptor (PYR1-like) PYL displayed downregulation in P2 compared to its level in P1. Lastly, we identified five genes encoding the BRI1 KINASE INHIBITOR1 (BKI1), the majority of which exhibited high expression levels in P1.

Clustering and functional analysis of DEGs

A total of 9,449 DEGs were identified across the four developmental stages and were categorized into six clusters based on their expression patterns (Fig. 4A). Cluster 3 (comprising 1,598 genes) and cluster 3 (comprising 1,245 genes) exhibited high expression levels in P3. Genes in cluster 2 (comprising 1,489 genes) and cluster 5 (comprising 1,231 genes) were predominantly expressed in P4 and P2, respectively. On the other hand, cluster 1 (comprising 1,888 genes) and cluster 4 (comprising 1,998 genes) displayed similar decreasing trends with higher expression in P1. Additionally, it is worth noting that TFs play a crucial role in the regulation of axillary bud outgrowth. Among Cluster 1 and Cluster 4, we identified a total of 461 TFs distributed across 49 TF families. The most prominent family was bHLH, comprising 47 members, followed by ERF (43 members), NAC (43 members), MYB (42 members), G2-like (27 members), and C2H2 (24 members) (Fig. 4B). Furthermore, we also identified seven TCP genes in this analysis.

Validation of RNA-Seq by qRT-PCR

To ascertain the accuracy of the RNA-seq data, nine DEGs known to be associated with axillary bud outgrowth in other species were chosen for qRT-PCR analysis. These DEGs exhibited parallel expression patterns in both the qRT-PCR and RNA-seq results. Correlation analysis revealed a robust positive correlation ($R^2 > 0.91$) between the qRT-PCR and RNA-seq data for these DEGs, affirming the reliability of the transcriptome data (Fig. S3).

Molecular cloning and bioinformatic analysis of *LhCYCL* and its promoter

One of the *TCP* genes, identified as *CYC-like* in the axillary bud transcriptome, emerged as a promising candidate for regulating axillary bud development. The CDS of this gene spanned 1,278 bp, encoding a protein comprising 425 amino acids (PP067739). A BlastP analysis of the hybrid *Liriodendron* CYCL protein demonstrated a substantial sequence similarity, with a remarkable 91.98% identity and 99% query coverage, to the *Magnolia sinica* CYC-like protein (XP_058078983). Notably, LhCYCL featured a conserved TCP domain (basic helix-loop-helix) and an R domain, akin to other CYC-like proteins (Fig. 5A). Phylogenetic analysis delineated distinct clades for CYC proteins, categorizing them as CYC1, CYC2, CYC3, dicotyledons CYC-like, and monocotyledons TB1-like. Within this phylogenetic tree, LhCYCL clustered within the dicotyledons CYC-like clade, with its closest relation being the *Magnolia sinica* CYC-like protein (Fig. 5B). Moreover, predictive analysis suggested the nuclear localization of the LhCYCL protein.

A 2,000 bp sequence located upstream of the translational initiation site (ATG) of the *LhCYCL* gene was isolated from hybrid *Liriodendron* leaves. The sequence analysis revealed the presence and distribution of putative cis-acting elements within *LhCYCLpro*, as shown in Fig. 5C. In addition to fundamental cis-acting elements like the TATA-box and CAAT-box, *LhCYCLpro* also featured various hormone-responsive elements, encompassing gibberellin-responsive elements (GARE-motif and P-box), an auxin-responsive element (AuxRR-core), abscisic acid-responsive elements (ABRE), and a salicylic acid-responsive element (TCA-element). Furthermore, light-responsive elements (G-Box and G-box), low-temperature-responsive elements (LTR), and regulating meristem expression elements (CAT-box) were also discernible within *LhCYCLpro*.

Expression patterns analysis of *LhCYCL*

The qRT-PCR analysis unveiled differential expression patterns of *LhCYCL* across various tissues in hybrid *Liriodendron*. The highest expression levels were observed in

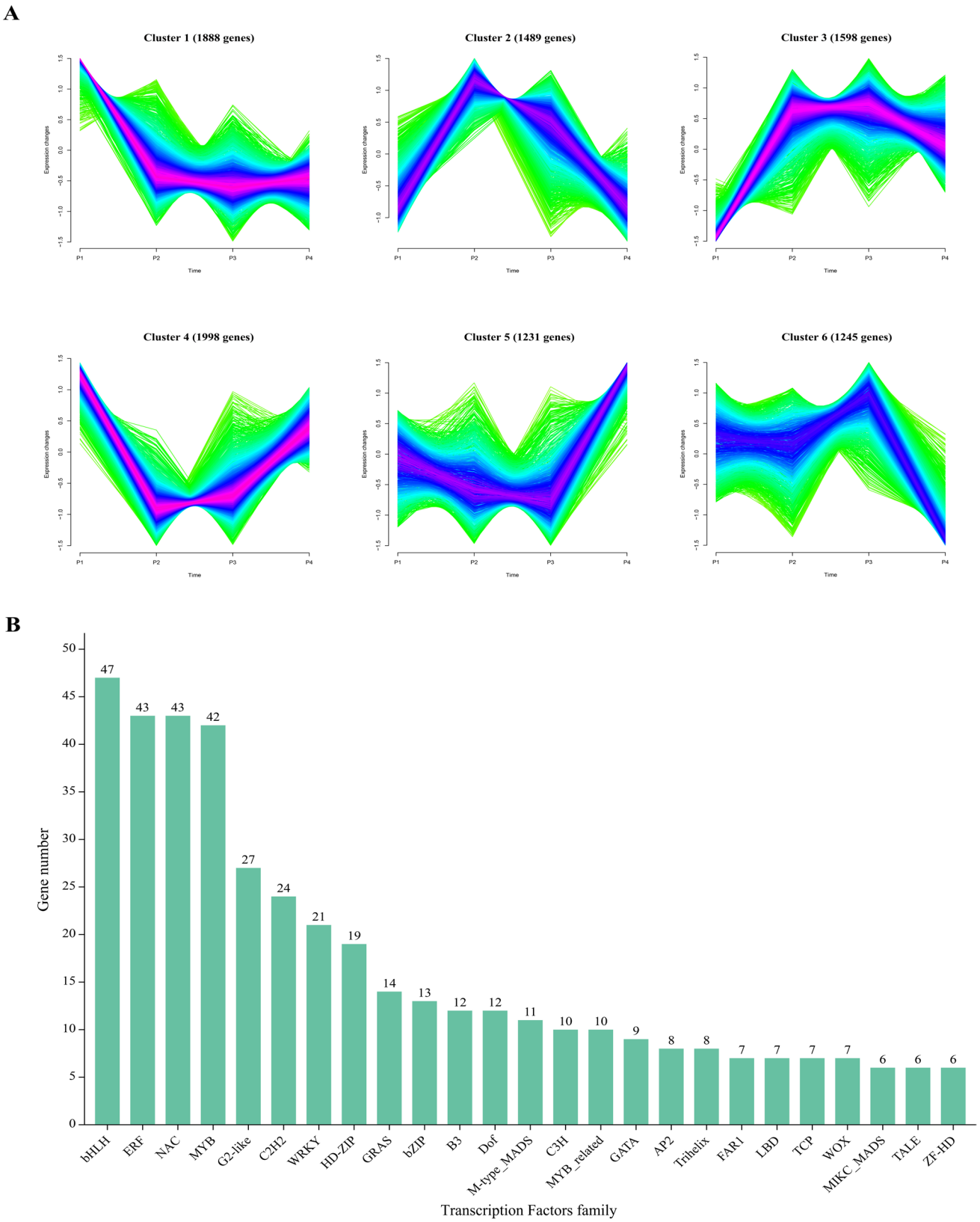

Fig. 4 Expression patterns and functional analysis of DEGs during the whole development period from P1 to P4. **A** Cluster analysis of DEGs. **B** Analysis of TF families among Cluster 1 and 4

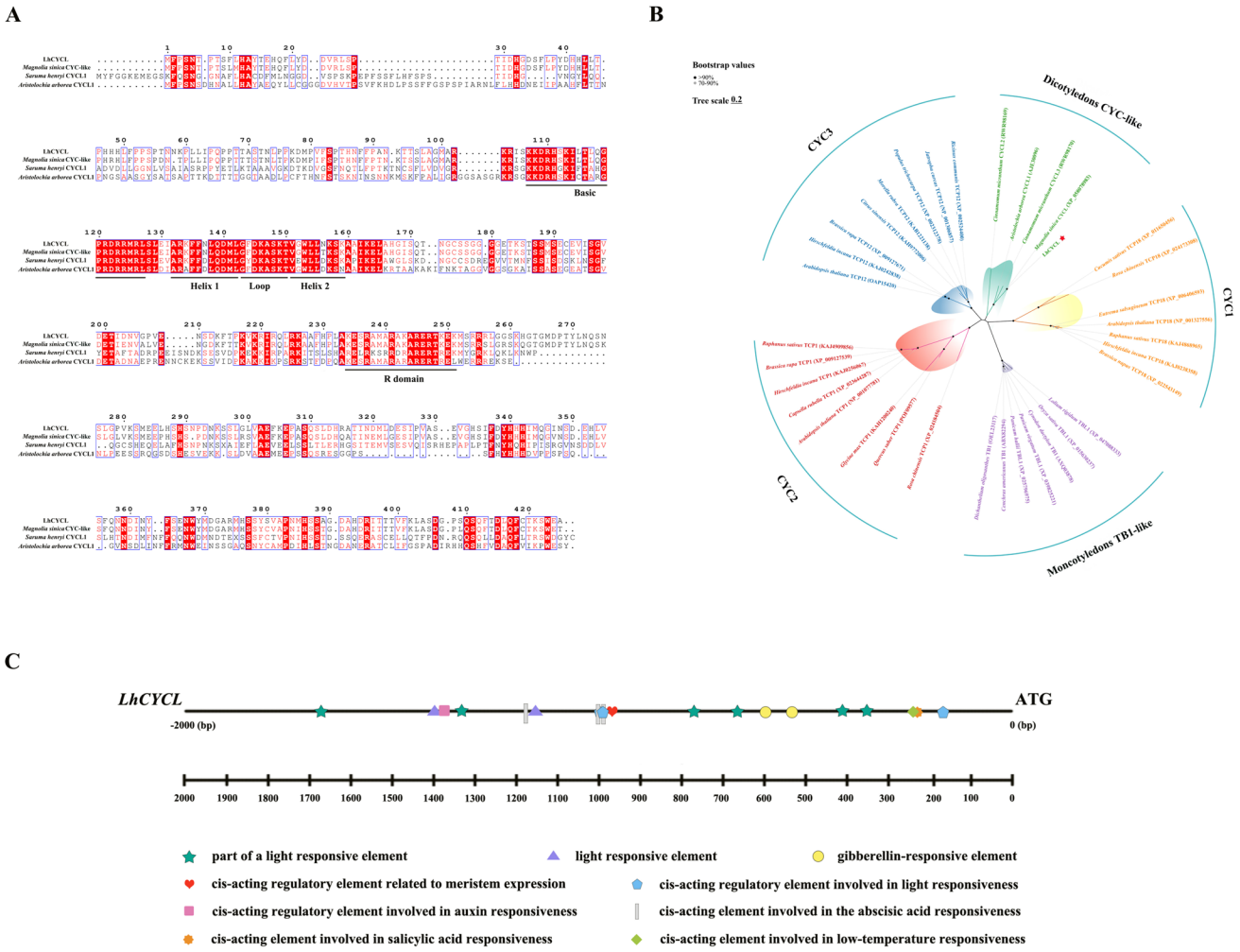

Fig. 5 Sequence analysis of the LhCYCL. **A** Amino acid alignment of CYCL proteins among hybrid *Liriodendron* and other plants. **B** Phylogenetic analysis of CYC/TB1 proteins from hybrid *Liriodendron* and selected other species. **C** The cis-elements analysis of *LhCYCL* promoter

the axillary bud, followed by the apical bud, flower bud, root, stem, and leaf, with comparatively lower expression levels in the pistil. Conversely, expression levels were notably lower in the sepal, petal, and stamen (Fig. 6A). To gain further insights into the expression pattern of *LhCYCL*, we generated *A. thaliana* reporter lines carrying the *LhCYCLpro::GUS* construct. In 30-day-old transgenic seedlings, GUS staining was primarily concentrated in the axils of cauline leaves and vascular tissue (Fig. 6B). Notably, there was more pronounced staining at the leaf axils.

Confocal microscopy examination provided additional evidence supporting the nuclear localization of LhCYCL. The fluorescence signal of the LhCYCL::GFP fusion protein overlapped with the nuclear marker, confirming our earlier predictions (Fig. 6C).

Ectopic expression of *LhCYCL* in *A. thaliana*

Following HygB screening, we successfully isolated 20 independent T_1 lines of transgenic *A. thaliana* plants that overexpressed *LhCYCL* under the control of the CaMV 35S promoter, hereafter referred to as *35S::LhCYCL*. These lines were further characterized through PCR amplification. Subsequently, 10 T_1 lines displaying consistent phenotypes were subjected to qRT-PCR analysis. Among them, Line 5 exhibited the highest level of *LhCYCL* expression, followed by Line 2 and Line 14 (Fig. 7A). Consequently, we selected the corresponding homozygous T_3 lines of *35S::LhCYCL A. thaliana* plants (Line 2, Line 5, and Line 14) for further investigations.

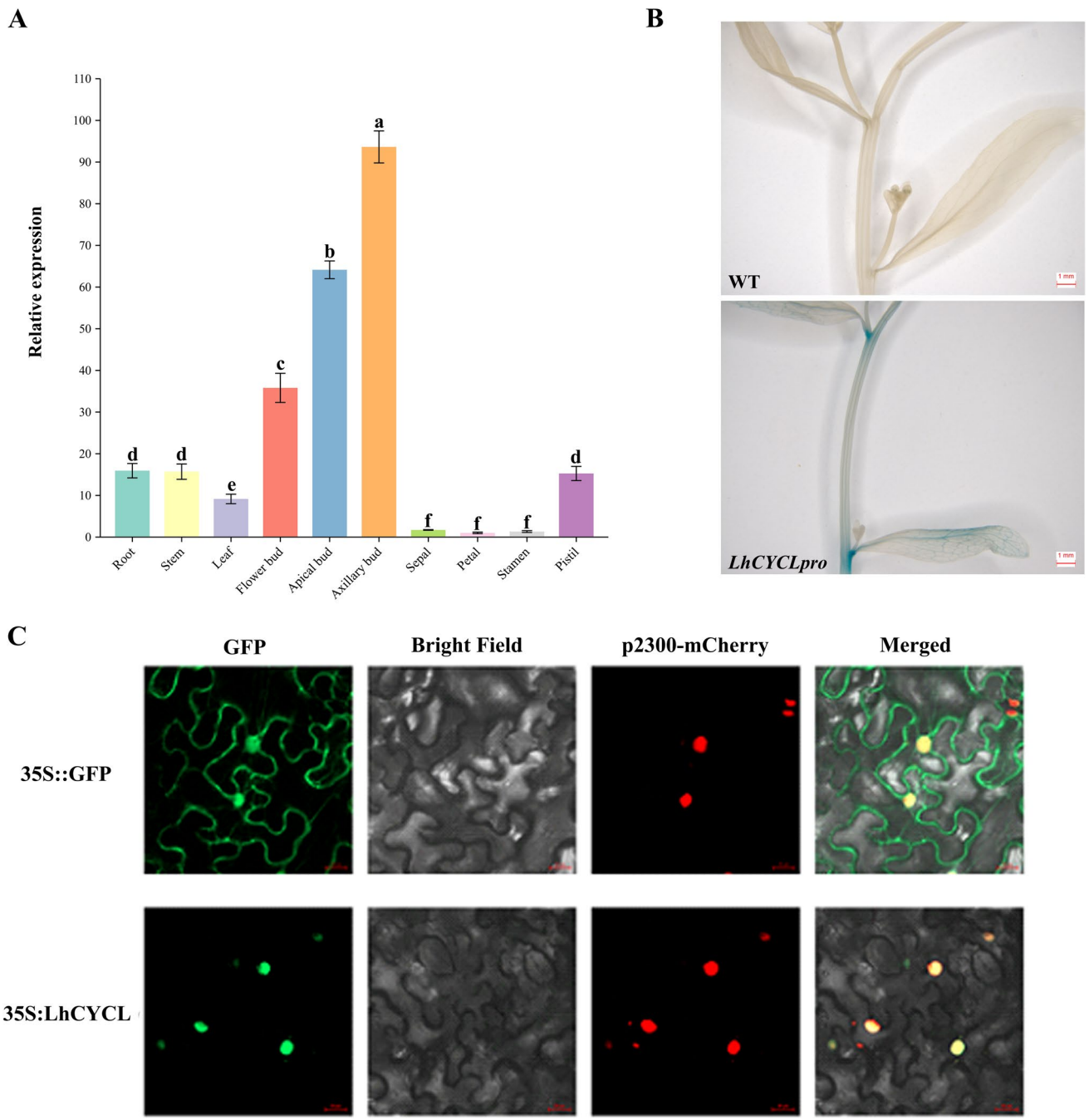

Fig. 6 Expression patterns analysis of *LhCYCL*. **A** Relative expression levels of *LhCYCL* in different organs of hybrid *Liriodendron*. **B** Histochemical analysis of GUS in WT and transformed *A. thaliana* plants, bars = 1 mm. **C** Subcellular location analysis of LhCYCL protein in leaf epidermal cells. The 35S::GFP served as the positive control. Green fluorescence indicates the GFP fusion protein signal, while red fluorescence indicates the nucleus marker p2300-mCherry. Yellow represents the merged signals. Bars = 20 μm

Overexpression of *LhCYCL* had a profound impact on the growth and development of transgenic plants (Fig. 7B). The average leaf area of *35S::LhCYCL-Line2*, *35S::LhCYCL-Line5*, and *35S::LhCYCL-Line14* measured 61.21 mm^2, 61.86 mm^2, and 62.34 mm^2, respectively, which was significantly smaller than that of the WT plants (328.99 mm^2) (Fig. 7C, D). Furthermore, the plant height of *35S::LhCYCL* transgenic plants was considerably reduced, with WT plants reaching 30.51 cm, whereas Line 2, Line 5, and Line 14 only reached 3.91 cm, 4.11 cm, and 3.9 cm, respectively (Fig. 7E, F). Most notably, *35S::LhCYCL-Line2*, *35S::LhCYCL-Line5*, and *35S::LhCYCL-Line14* at 50 days of growth

produced an average of 3, 2.9, and 2.8 rosette branches, respectively, while WT plants produced only 1.3 branches (Fig. 7E, G). Moreover, the three *35S::LhCYCL* transgenic lines produced an average of 5.2–5.9 secondary branches, significantly more than the 2.2 observed in WT plants (Fig. 7E, H). In summary, the heterologous expression of *LhCYCL* led to reductions in leaf area, plant stature, and an increase in branching in transgenic plants.

LhCYCL modulates the expression of genes associated with plant hormone signal pathway

As is well-established, CK play a pivotal role in promoting shoot branching. The *35S::LhCYCL* transgenic lines exhibited higher levels of ZT compared to the WT *A. thaliana* plants (Fig. 8A). Moreover, we conducted an assessment of the expression levels of genes related to CK biosynthesis and signaling in both WT and *LhCYCL*-overexpressing *A. thaliana* plants. The results presented that the transcript levels of CK biosynthetic genes (including *AtIPT1*, *AtIPT3*, *AtIPT6*, *AtIPT7*, and *AtIPT9*) and CK signaling genes (comprising *AtAHK3*, *AtAHK4*, *AtARR1*, *AtARR3*, *AtARR4*, *AtARR7*, *AtARR10*, and *AtARR12*) were significantly higher in *LhCYCL*-overexpressing plants compared to WT *A. thaliana* plants (Fig. 8B). Furthermore, overexpression of *LhCYCL* resulted in the downregulation of *AtBRC1* and the upregulation of *AtWUS*.

In parallel, we have detected the relative expression level of some genes involved in auxin, GA, ABA, and BR signal transduction in both WT and transgenic plants. The results demonstrated that the transcript levels of auxin signaling genes (including *AtARF8*, *AtARF10*, and *AtARF15*) and ABA signaling gene (*AtSnRK2.3*) were significantly lower in *LhCYCL*-overexpressing plants compared to WT *A. thaliana* plants. Additionally, the overexpression of *LhCYCL* resulted in the upregulation of ABA signaling genes (*AtHAI1* and *AtPP2CA*) and BR signaling genes (*AtBZR1* and *AtBES1*). However, the expression levels of GA signaling genes *DELLAs* (including *AtRGL1*, *AtRGL3*, *AtRGA*, and *AtGAI*), exhibited no significant difference between WT and *LhCYCL*-overexpressing plants, as depicted in Fig. 9.

Discussion

Shoot branching is a crucial trait that significantly influences both the yield and quality of wood in woody plant species. Hybrid *Liriodendron*, known for its rapid growth and diverse applications, is a valuable timber species. Nevertheless, our understanding of the underlying mechanisms governing shoot branching development in hybrid *Liriodendron* remains limited. RNA-seq technology offers a valuable tool for assessing gene expression across various plant physiological conditions, allowing us to uncover the molecular components within tissues and cells (Wang et al. 2009). In this study, we conducted transcriptome sequencing across different developmental stages of axillary buds, aiming to elucidate potential genes involved in the regulation of shoot branching. This research forms a solid foundation for understanding the molecular mechanisms governing shoot branching in hybrid *Liriodendron*.

LhCYCL has the specific function in shoot branching

LhCYCL demonstrated prominent expression in the axillary buds (Fig. 6A), akin to *TCP62*, *HaTCP1*, and *CsBRC1-like* genes, which also exhibit their highest expression levels in buds (Liu et al. 2021; Shen et al. 2021; Wu et al. 2023). Notably, the *LhCYCLpro* contains cis-acting regulatory elements associated with meristem expression (Fig. 5C), suggesting a potential role in modulating meristem activity. As we are aware, axillary meristems are located in leaf axils, and strong GUS activity was observed in the leaf axils of transgenic *A. thaliana* cauline leaves (Fig. 6B). These results further support the hypothesis that *LhCYCL* may contribute to axillary bud growth, a notion substantiated by the increased branching observed in *35S::LhCYCL* transgenic plants (Fig. 7E, G, H).

In a phylogenetic analysis of CYC/TB1 clade genes conducted by Citerne *et al.*, CYC/TB1 genes were classified into Monocot CYC/TB1-like, CYC1, CYC2, CYC3, and Basal eudicot CYC-like clades (Citerne et al. 2013). In *A. thaliana*, TCP18, TCP1, and TCP12 belong to the CYC1, CYC2, and CYC3 clades respectively. Citerne *et al.* have found that up to three other regions of the *A. thaliana* genome shared several genes syntenic with the CYC loci, but were missing *CYC-like* genes, which indicated there is no *CYC-like* gene in *A. thaliana* (Citerne et al. 2013). Phylogenetic analysis revealed that LhCYCL clustered in the dicotyledons CYC-like clade, and not belonging to the CYC1, CYC2, CYC3, and monocotyledons TB1-like clade (Fig. 5B). Furthermore, the sequence homology between LhCYCL and CYC1/2/3 was notably low. The above results indicated that the LhCYCL is not homologous to the CYC1/2/3 and it may serve distinct functions separate from CYC1/2/3 found in other plants. While the overexpression of *MdTCP12* and *CsBRC-like* genes has been shown to negatively regulate the total number of branches (Li et al. 2021; Shen et al. 2021), there is currently no literature reporting that *CYC-like* genes promote shoot branching. Most *CYC-like* genes are recognized for their roles in regulating floral development. For instance, in *Scrophulariaceae* and *Gesneriaceae* species, *CYC-like* genes predominantly influence the morphological traits of stamen and petal development (Chai et al. 2023). In *Fabaceae* species, *CYC-like* genes are associated with the

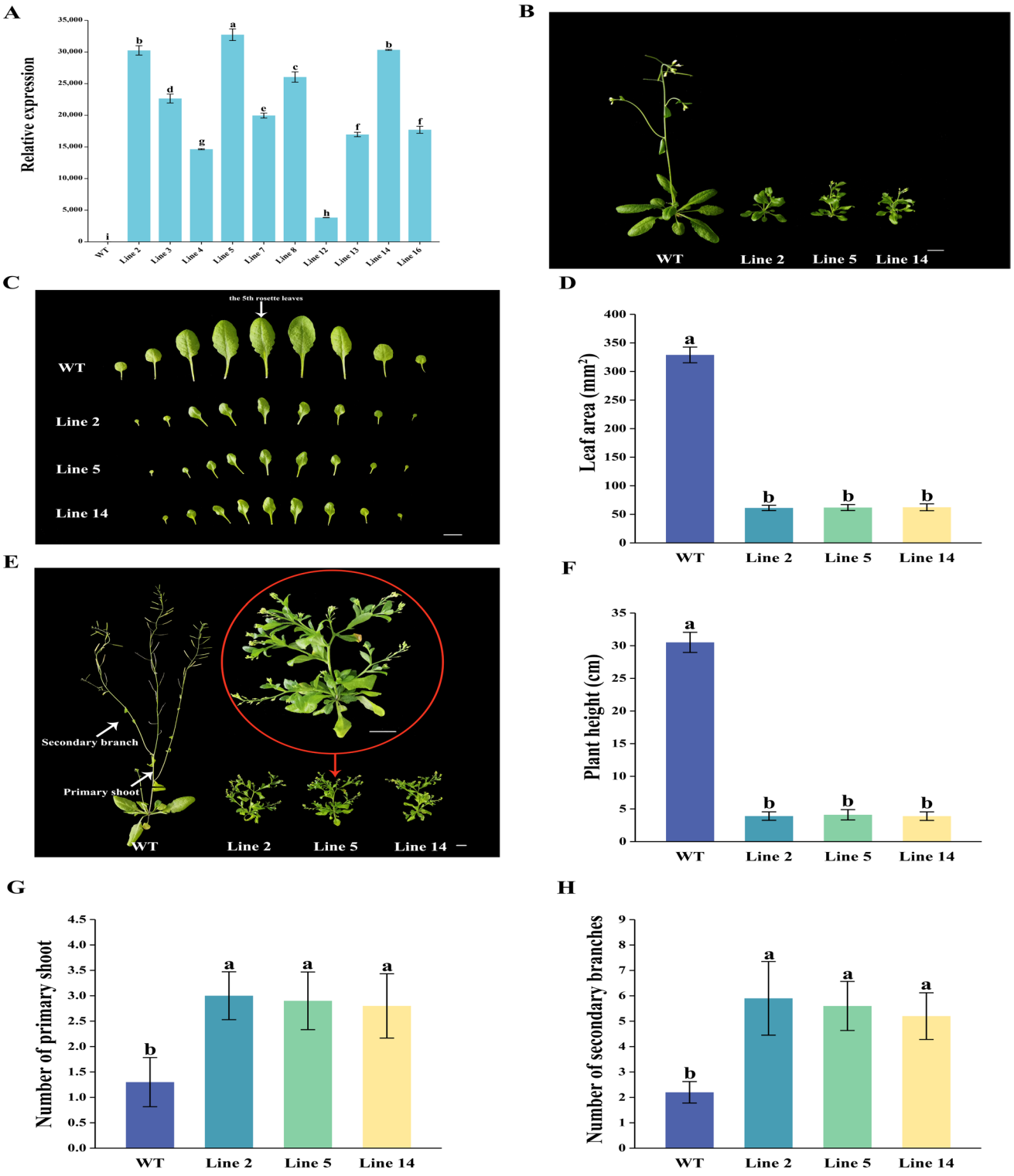

regulation of floral symmetry (Citerne et al. 2006), while in *Asteraceae* species, they play a role in regulating morphological changes in capitulum (Broholm et al. 2008). These findings indicate that the *LhCYCL* may play a novel role in regulating shoot branching compared to its homologous genes in other species.

Functional analysis of the conserved TCP domain in LhCYCL

LhCYCL possesses both the TCP domain and the R domain, as evident from sequence alignment (Fig. 5A). The TCP domain is highly conserved across plant species, featuring

◂**Fig. 7** Overexpressing *LhCYCL* promotes the shoot branching in *A. thaliana*. **A** RT-qPCR analysis of *LhCYCL* expression levels in WT and positive transgenic plants, *Actin2* was used as a reference gene. Values are means ± SD (n = 3). Data are based on three independent experiments. **B** The phenotype of WT and transgenic *A. thaliana* plants at 30 days after transplantation, bar = 1 cm. **C** Morphological characteristics of rosette leaves of 30-day-old transgenic and WT *A. thaliana*, bar = 1 cm. **D** Area of 5th rosette leaves in 30-day-old transgenic and WT *A. thaliana*. Values are means ± SD (n = 10). **E** Phenotype of WT and transgenic *A. thaliana* plants at 50 days after transplantation, bars = 1 cm. **F** Plant height of 50-day-old transgenic and WT *A. thaliana*. Values are means ± SD (n = 10). **G** Number of primary shoots in 50-day-old transgenic and WT *A. thaliana*. Values are means ± SD (n = 10). **H** Number of secondary branches in 50-day-old transgenic and WT *A. thaliana*. Values are means ± SD (n = 10). For statistical analyses, one-way ANOVA and Duncan test were used. In A, D, F, G, and H, different lowercase letters above the bars represent significant differences ($P < 0.05$)

a bHLH secondary structure comprised of approximately 58 to 62 amino acid residues. This domain is known to play essential roles in DNA binding, protein–protein interactions, and nuclear localization (Zhou et al. 2022). Notably, TCP proteins within the same class across different species recognize conserved DNA binding sequences (GGNCCCAC for class I and GTGGNCCC for class II) (Kosugi and Ohashi 2002). LhCYCL falls into class II, suggesting the potential to identify genes regulated by LhCYCL using the known DNA binding sequence. Research has revealed that the TCP domain, with its conserved amphipathic helices, facilitates protein–protein interactions (Pruneda-Paz et al. 2009). In fact, all three CYC/TB1 proteins in *A. thaliana* can interact with each other, and sunflower's HaCYC1a and HaCYC1b proteins can form heterodimers (Tahtiharju et al. 2012). Further investigations are warranted to elucidate the interactions between LhCYCL and other CYC/TB1 proteins in hybrid *Liriodendron*. Subcellular localization results corroborate that LhCYCL is situated within the nucleus (Fig. 6C), prompting speculation that the bHLH secondary structure may be linked to LhCYCL localization. Recent reports have highlighted the contrasting functions of rice *OsTb1* and its closest paralog, *OsTb2*, in governing inflorescence development (Lyu et al. 2020). Additionally, Mansilla et al. demonstrated that an adaptive site within the TCP domain potentially facilitated neo-functionalization within the CYC/TB1-like clade by modulating interactions with chromatin (Mansilla et al. 2023). This is one of the reasons why *LhCYCL* exhibits the function of promoting shoot branching.

LhCYCL may promote the shoot branching by regulating the plant hormone signaling

CKs play a crucial role in promoting shoot branching by directly activating axillary buds (del Rosario et al. 2022). Du *et al.* have substantiated this by demonstrating how *UNBRANCHED3* (*UB3*) modulates branching patterns through the regulation of CK biosynthesis and signaling (Du et al. 2017). Moreover, the hybrid aspen *LAP1* promotes shoot branching in a CK-dependent manner (Maurya et al. 2020). Several studies have shown that increased expression of *IPT* genes contributes to axillary bud growth (Ferguson and Beveridge 2009; Li et al. 2018), with heterologous overexpression of *MdRR9* (type-A ARR) resulting in increased lateral branches in tomatoes (Zhao et al. 2023). Additionally, ovexpression of *J. curcas JcRR12* (type-B ARR) in *A. thaliana* led to a slight increase in the number of rosette branches after decapitation (Geng et al. 2022). A higher content of ZT was observed in the *35S::LhCYCL* plants than WT *A. thaliana* plants (Fig. 8A). Therefore, we hypothesize that *LhCYCL* promotes CK biosynthesis by enhancing the expression of *IPT* genes in transgenic *A. thaliana* plants. Additionally, *BRC1* is a key gene that inhibits shoot branching, and the downregulation of *BRC1* leads to branch outgrowth (Aguilar-Martínez et al. 2007). To an extent, CK could regulate shoot branching by negatively regulating the expression of *BRC1* (Braun et al. 2012). Furthermore, the transcript levels of *Oryza sativa TB1/FC1* and *Chrysanthemum morifolium BRC1* reduced in a CK-dose-dependent manner (Minakuchi et al. 2010; Dierck et al. 2016). Based on the available data, we speculate that the augment of CK levels result in the downregulation of *AtBRC1*, thereby promoting shoot branching in transgenic *A. thaliana*.

CK can also induce the expression of type-A ARRs, resulting in an increase in the expression level of type-A ARRs in *35S::LhCYCL* plants. *ARABIDOPSIS HISTIDINE KINASE 3* (*AHK3*) and *AHK4* function as CK receptors in the CK-signaling pathway (Yamada et al. 2001). Heterologous expression of *LhCYCL* upregulated the expression of *AtAHK3* and *AtAHK4* in transgenic *A. thaliana* plants (Fig. 8B). Moreover, type-B ARRs have been identified as key signaling components downstream of *AHKs* (Yokoyama et al. 2007). This suggests that *LhCYCL* may indirectly induce the expression of *AtAHK3* and *AtAHK4* by increasing CK levels in transgenic *A. thaliana* plants, thereby promoting the expression of *ARR1/10/12*. Additionally, Wang et al. reported that *ARR1/10/12* can bind to the promoter of *WUS* to activate its expression, contributing to the axillary meristem initiation (Wang et al. 2017). Overexpression of *MdWUS2* could lead to increased branching in *A. thaliana* (Li et al. 2021). *Populus PtrTALE12* promotes the development of axillary buds by regulating the expression of *WUS* (Bae et al. 2020). In this study, heterologous expression of *LhCYCL* upregulated the expression of *AtWUS* in transgenic *A. thaliana* plants (Fig. 8B), suggesting that *LhCYCL* may induce the expression of *WUS* by upregulating the expression of type-B ARRs, thereby promoting shoot branching in transgenic *A. thaliana* plants. The above results indicate

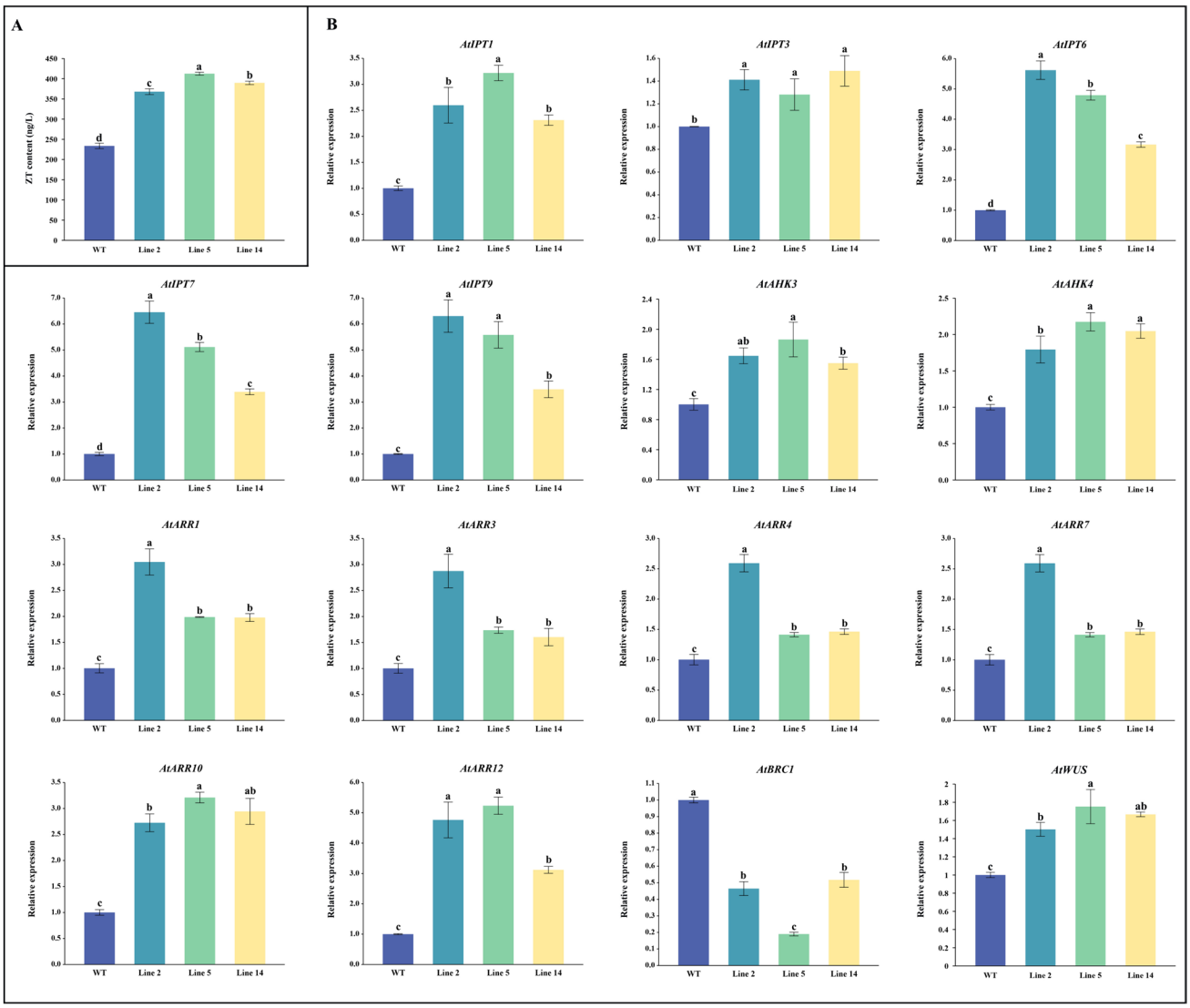

Fig. 8 *LhCYCL* upregulates the expression of CK biosynthesis and signaling. **A** The ZT concentration of WT and transgenic *A. thaliana* plants. **B** *LhCYCL* promotes shoot branching in *A. thaliana* by modulating the expression of CK biosynthesis, CK signaling, and shoot branching-related genes. The *A. thaliana Actin2* was used as a reference gene. All data presented are the means ± SD obtained from three repetitive experiments. For statistical analyses, one-way ANOVA and Duncan test were used. Different lowercase letters above the bars indicate significant differences ($P < 0.05$)

that *LhCYCL* regulation of shoot branching likely involves the CK signaling pathway.

KEGG enrichment analysis has highlighted the potential significance of 'Plant hormone signal transduction' in regulating axillary bud development in hybrid *Liriodendron* (Fig. 3). Recent research has revealed that low red light: far red light inhibits branching by promoting auxin signaling (Holalu et al. 2021). Furthermore, *SlARF2a* acts as a negative regulator in axillary bud formation (Xu et al. 2016). These findings collectively indicated that auxin signaling exerts a suppressive impact on shoot branching. Therefore, it is plausible that *LhCYCL* promotes shoot branching by inhibiting the expression levels of auxin signal transduction genes in transgenic *A. thaliana* plants. Moreover, DELLA proteins function as inhibitors in the GA signal pathway. The interplay between DELLA protein and SPL9 diminishes SPL9's inhibitory effect on *LAS*, thereby fostering the formation of axillary buds (Zhang et al. 2020). Overexpression of *LhCYCL* did not induce the expression of *DELLAs* in transgenic *A. thaliana* plants, indicating that the regulation of shoot branching by *LhCYCL* may not involve the GA signal pathway. Group A protein type 2C phosphatases (PP2Cs) serve as negative regulators of ABA signaling, and overexpression of potato group A PP2C *StHAB1* promotes axillary bud outgrowth (Liu et al. 2023). In this study, overexpression of *LhCYCL* upregulates the negative regulator

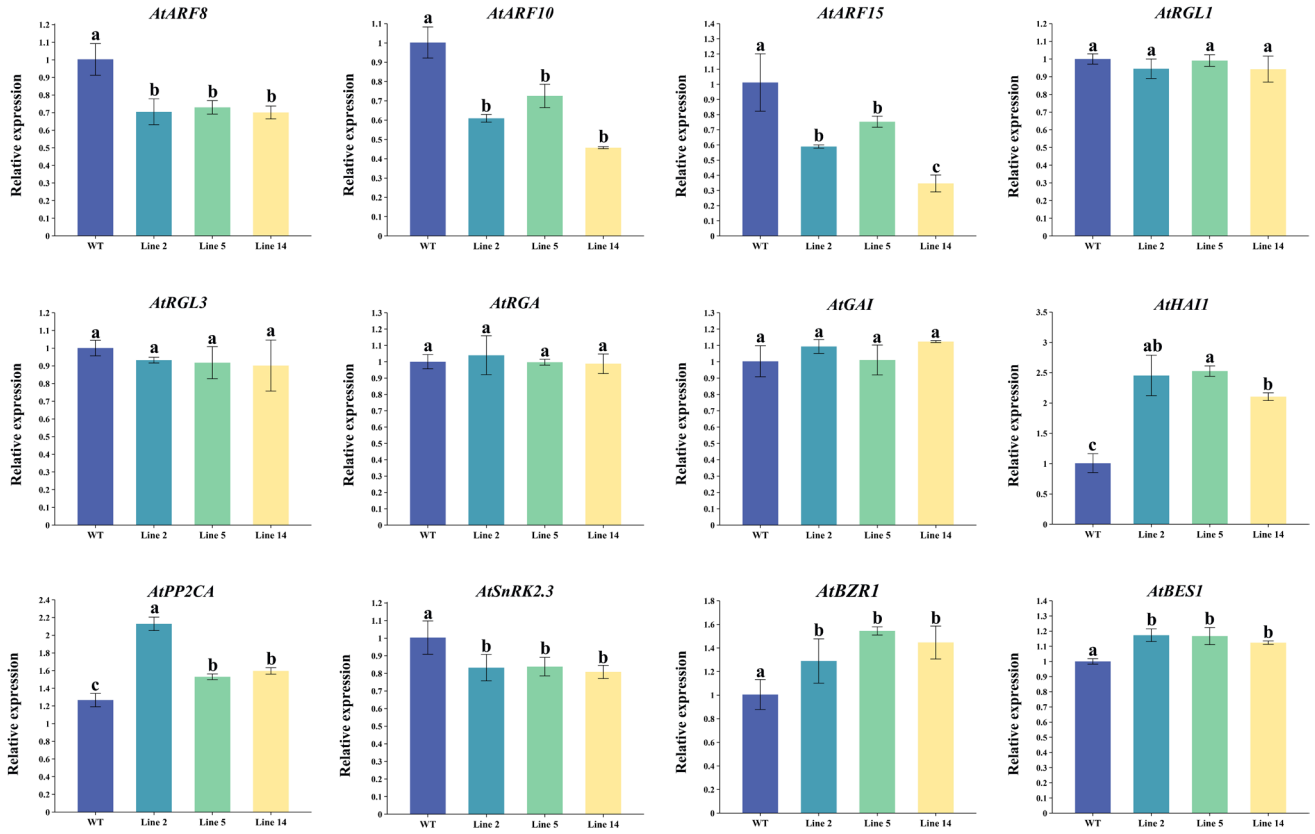

Fig. 9 *LhCYCL* modulates the expression of genes involved in auxin, ABA, GA, and BR signal transduction. The *A. thaliana Actin2* was used as a reference gene. All data presented are the means ± SD obtained from three repetitive experiments. For statistical analyses, one-way ANOVA and Duncan test were used. Different lowercase letters above the bars indicate significant differences ($P < 0.05$)

factors (*AtHAI1* and *AtPP2CA*) and downregulates the positive regulator (*AtSnRK2.3*) in the ABA signal pathway, suggesting that *LhCYCL* may also promote shoot branching by inhibiting ABA signaling. In addition, *BZR1* mediates BR to promote axillary bud outgrowth in tomato through the direct suppression of *BRC1* (Xia et al. 2021). Consequently, *LhCYCL* may stimulate branching in transgenic *A. thaliana* plants by supressing the expression of *BRC1* through the promotion of BR signaling transduction. Above all, *LhCYCL* may integrate multiple hormone signal pathways to regulate the shoot branching.

In fact, some genes involved in the hormone signal transduction, such as *ARF*, *ARR*, *DELLA*, *PP2C*, *SnRK2* genes, are differential expressed during the axillary bud growth in hybrid *Liriodendron*, indicating their potential roles in regulating shoot branching. However, there is no clear experimental evidence to suggest that their direct involvement in the regulation of hybrid *Liriodendron* shoot branching. The potential regulatory roles of these plant hormone signal transduction genes on shoot branching of hybrid *Liriodendron* warrant further study.

As mentioned before, the class II TCP proteins from different species can recognize conserved DNA binding sequence (GTGGNCCC) (Kosugi and Ohashi 2002). *LhCYCL* may bind to the DNA sequence on the promoter of plant hormone signaling genes, directly regulating their expression. The identification and validation of *LhCYCL*'s target genes are essential for a comprehensive understanding of how *LhCYCL* regulates shoot branching in hybrid *Liriodendron* through the hormone signal pathway. Moreover, Tahtiharju et al. have proved that CYC/TB1 proteins in *A. thaliana* can interact with each other (Tahtiharju et al. 2012). BRC1 has the ability to directly bind to *HB21*, *HB40*, and *HB53* and positively regulate their transcription, leading to local ABA accumulation and subsequently inhibiting axillary bud outgrowth (González-Grandío et al. 2017). CsBRC1 directly inhibits the expression of the *CsPIN3*, reducing the accumulation of auxin in axillary buds and inhibiting the axillary bud outgrowth (Shen et al. 2019). Hence, LhCYCL may interact with other CYC/TB1 proteins or unknown proteins, indirectly regulate the expression of plant hormone signaling genes.

In addition, the regulatory mechanisms underlying axillary bud outgrowth are governed by a sophisticated network of plant hormones. Plant hormones can interact with each other and ultimately regulate shoot branching. For

instance, auxin reduces the CK content in axillary buds by inhibiting the expression of *IPT* and promoting the expression of *CKX* (Shimizu-Sato et al. 2009). Overexpression of the *CKX2* gene can lead to excessive growth of tomato axillary buds, where CK regulates axillary bud growth by reducing auxin transport (Pino et al. 2022). Additionally, CK can promote the synthesis of BR in axillary buds through the *ARR10* (Xia et al. 2021). Ni *et al.* have revealed that gibberellin A3 (GA3) and 6-benzyladenine (BA, a synthetic CK) cooperatively regulate axillary bud outgrowth in *J. curcas* (Ni et al. 2017). Moreover, Geng *et al.* believed that the promotion of axillary bud outgrowth by GA in *J. curcas* is dependent on CK (Geng et al. 2022). Researchers have uncovered that the status of axillary buds in apple may be determined by combined relative strength of CK signaling, SL, and auxin transport in axillary buds (Tan et al. 2019). It can be speculated that *LhCYCL* may indirectly influence the expression of other plant hormone-related genes by regulating the expression of certain hormone biosynthesis or signaling genes. Further exploration is needed to elucidate whether *LhCYCL* regulates the shoot branching of hybrid *Liriodendron* through a specific single signaling pathway or by integrating multiple plant hormone signaling pathways.

These results collectively suggest that *LhCYCL* may play a pivotal role in the axillary bud development of hybrid *Liriodendron*. It can be hypothesized that knocking out *LhCYCL* might inhibit shoot branching in hybrid *Liriodendron*, contributing to enhanced timber quality. Our future work will focus on the knockout of *LhCYCL* in hybrid *Liriodendron* to observe phenotypic and gene expression changes resulting from this genetic modification.

Supplementary Information The online version contains supplementary material available at https://doi.org/10.1007/s11103-024-01458-5.

Acknowledgements The authors thank their laboratory colleagues for their help in lab work, including Zhonghua Tu, Lichun Yang, Hainan Wu, Lingming Wei, Yaxian Zong, Yanqing Zhao, Chengge Zhang, Muju Liu, Wei Li, Zhengkun Cui, Junpeng Wu, Xinyu Zhai, Yu Zhang, and Minxin Wang.

Author contributions Shaoying Wen designed the experiment, conducted the experiments, and wrote the manuscript. Qinghua Hu took part in the RNA extraction and plasmid construction. Jing Wang is involved in the collection of plant materials. Huogen Li conceived the project and revised the manuscript. All authors have read and approved the final manuscript.

Funding This work was supported by the National Research and Development Program (2022YFD2200104), the National Natural Science Foundation of China (32371910, 31770718), and the Priority Academic Program Development of Jiangsu Higher Education Institutions (PAPD).

Data availability The data that support the findings of this study are available from the corresponding authors upon reasonable request.

Declarations

Conflict of interest The authors declare that they have no competing interests.

References

Aguilar-Martínez JA, Cs PC, Cubas P (2007) *Arabidopsis* branched1acts as an integrator of branching signals within axillary buds. Plant Cell 19:458–472. https://doi.org/10.1105/tpc.106.048934

An J, Guo Z, Gou X, Li J (2011) TCP1 positively regulates the expression of DWF4 in *Arabidopsis thaliana*. Plant Signal Behav 6:1117–1118. https://doi.org/10.4161/psb.6.8.15889

Bae S, Kim M, Cho J, Park E, Lee H, Kim J, Ko J (2020) Overexpression of populus transcription factor PtrTALE12 increases axillary shoot development by regulating WUSCHEL expression. Tree Physiol 40:1232–1246. https://doi.org/10.1093/treephys/tpaa062

Barbier F, Peron T, Lecerf M, Perez-Garcia MD, Barriere Q, Rolcik J, Boutet-Mercey S, Citerne S, Lemoine R, Porcheron B, Roman H, Leduc N, Le Gourrierec J, Bertheloot J, Sakr S (2015) Sucrose is an early modulator of the key hormonal mechanisms controlling bud outgrowth in rosa hybrida. J Exp Bot 66:2569–2582. https://doi.org/10.1093/jxb/erv047

Barbier F, Dun E, Kerr S, Chabikwa T, Beveridge C (2019) An update on the signals controlling shoot branching. Trends Plant Sci 24:220–236. https://doi.org/10.1016/j.tplants.2018.12.001

Bolger AM, Lohse M, Usadel B (2014) Trimmomatic: a flexible trimmer for illumina sequence data. Bioinformatics 30:2114–2120. https://doi.org/10.1093/bioinformatics/btu170

Braun N, de Saint GA, Pillot J-P, Boutet-Mercey S, Dalmais M, Antoniadi I, Li X, Maia-Grondard A, Le Signor C, Bouteiller N, Luo D, Bendahmane A, Turnbull C, Rameau C (2012) The pea TCP transcription factor PsBRC1 acts downstream of strigolactones to control shoot branching. Plant Physiol 158:225–238. https://doi.org/10.1104/pp.111.182725

Broholm SK, Tahtiharju S, Laitinen RAE, Albert VA, Teeri TH, Elomaa P (2008) A TCP domain transcription factor controls flower type specification along the radial axis of the Gerbera (Asteraceae) inflorescence. Proc Natl Acad Sci USA 105:9117–9122. https://doi.org/10.1073/pnas.0801359105

Chai Y, Liu H, Chen W, Guo C, Chen H, Cheng X, Chen D, Luo C, Zhou X, Huang C (2023) Advances in research on the regulation of floral development by CYC-like genes. Curr Issues Mol Biol 45:2035–2059. https://doi.org/10.3390/cimb45030131

Chatfield SP, Stirnberg P, Forde BG, Leyser O (2000) The hormonal regulation of axillary bud growth in *Arabidopsis*. Plant J 24:159–169. https://doi.org/10.1046/j.1365-313x.2000.00862.x

Chen J, Hao Z, Guang X, Zhao C, Wang P, Xue L, Zhu Q, Yang L, Sheng Y, Zhou Y, Xu H, Xie H, Long X, Zhang J, Wang Z, Shi M, Lu Y, Liu S, Guan L, Zhu Q, Yang L, Ge S, Cheng T, Laux T, Gao Q, Peng Y, Liu N, Yang S, Shi J (2019) Liriodendron genome sheds light on angiosperm phylogeny and species-pair differentiation. Nat Plants 5:18–25. https://doi.org/10.1038/s41477-018-0323-6

Citerne HL, Pennington RT, Cronk QCB (2006) An apparent reversal in floral symmetry in the legume Cadia is a homeotic transformation. Proc Natl Acad Sci USA 103:12017–12020. https://doi.org/10.1073/pnas.0600986103

Citerne HL, Le Guilloux M, Sannier J, Nadot S, Damerval C (2013) Combining phylogenetic and syntenic analyses for understanding the evolution of TCP ECE genes in *Eudicots*. PLoS ONE 8:e74803. https://doi.org/10.1371/journal.pone.0074803

Cline MG, Thangavelu M, Dong-Il K (2006) A possible role of cytokinin in mediating long-distance nitrogen signaling in the

promotion of sylleptic branching in hybrid poplar. J Plant Physiol 163:684–688. https://doi.org/10.1016/j.jplph.2005.06.005
Clough SJ, Bent AF (1998) Floral dip: a simplified method for Agrobacterium-mediated transformation of *Arabidopsis thaliana*. Plant J 16:735–743. https://doi.org/10.1046/j.1365-313x.1998.00343.x
del Rosario C-A, Sarria-Guzman Y, Martinez-Antonio A (2022) Review: isoprenoid and aromatic cytokinins in shoot branching. Plant Sci 319:111240. https://doi.org/10.1016/j.plantsci.2022.111240
Dierck R, De Keyser E, Riek J, Dhooghe E, Huylenbroeck J, Prinsen E, Van Der Straeten D (2016) Change in auxin and cytokinin levels coincides with altered expression of branching genes during axillary bud outgrowth in *Chrysanthemum*. PLoS ONE. https://doi.org/10.1371/journal.pone.0161732
Domagalska MA, Leyser O (2011) Signal integration in the control of shoot branching. Nat Rev Mol Cell Biol 12:211–221. https://doi.org/10.1038/nrm3088
Du Y, Liu L, Li M, Fang S, Shen X, Chu J, Zhang Z (2017) UNBRANCHED3 regulates branching by modulating cytokinin biosynthesis and signaling in maize and rice. New Phytol 214:721–733. https://doi.org/10.1111/nph.14391
Duan J, Yu H, Yuan K, Liao Z, Meng X, Jing Y, Liu G, Chu J, Li J (2019) Strigolactone promotes cytokinin degradation through transcriptional activation of CYTOKININ OXIDASE/DEHYDROGENASE 9 in rice. Proc Natl Acad Sci USA 116:14319–14324. https://doi.org/10.1073/pnas.1810980116
Faiss M, Zalubilova J, Strnad M, Schmulling T (1997) Conditional transgenic expression of the ipt gene indicates a function for cytokinins in paracrine signaling in whole tobacco plants. Plant J 12:401–415. https://doi.org/10.1046/j.1365-313X.1997.12020401.x
Ferguson BJ, Beveridge CA (2009) Roles for auxin, cytokinin, and strigolactone in regulating shoot branching. Plant Physiol 149:1929–1944. https://doi.org/10.1104/pp.109.135475
Fichtner F, Barbier FF, Feil R, Watanabe M, Annunziata MG, Chabikwa TG, Hoefgen R, Stitt M, Beveridge CA, Lunn JE (2017) Trehalose 6-phosphate is involved in triggering axillary bud outgrowth in garden pea (*Pisum sativum* L.). Plant J 92:611–623. https://doi.org/10.1111/tpj.13705
Geng X, Zhang C, Wei L, Lin K, Xu Z-F (2022) Genome-wide identification and expression analysis of cytokinin response regulator (RR) genes in the woody plant jatropha curcas and functional analysis of JcRR12 in Arabidopsis. Int J Mol Sci 23:11388. https://doi.org/10.3390/ijms231911388
González-Grandío E, Pajoro A, Franco-Zorrilla JM, Tarancón C, Immink RGH, Cubas P (2017) Abscisic acid signaling is controlled by a BRANCHED1/HD-ZIP I cascade in Arabidopsis axillary buds. Proc Natl Acad Sci 114:E245–E254. https://doi.org/10.1073/pnas.1613199114
Holalu SV, Reddy SK, Finlayson SA (2021) Low red light: far red light inhibits branching by promoting auxin signaling. J Plant Growth Regul 40:2028–2036. https://doi.org/10.1007/s00344-020-10253-7
Howarth DG, Donoghue MJ (2006) Phylogenetic analysis of the "'ECE" (CYC/TB1) clade reveals duplications predating the core *Eudicots*. Proc Natl Acad Sci USA 103:9101–9106. https://doi.org/10.1073/pnas.0602827103
Janssen BJ, Drummond RSM, Snowden KC (2014) Regulation of axillary shoot development. Curr Opin Plant Biol 17:28–35. https://doi.org/10.1016/j.pbi.2013.11.004
Katyayini NU, Rinne PLH, Tarkowska D, Strnad M, van der Schoot C (2020) Dual role of gibberellin in perennial shoot branching: inhibition and activation. Front Plant Sci 11:736. https://doi.org/10.3389/fpls.2020.00736
Kerr SC, Patil SB, de Saint GA, Pillot J-P, Saffar J, Ligerot Y, Aubert G, Citerne S, Bellec Y, Dun EA, Beveridge CA, Rameau C (2021) Integration of the SMXL/D53 strigolactone signalling repressors in the model of shoot branching regulation in *Pisum sativum*. Plant J 107:1756–1770. https://doi.org/10.1111/tpj.15415
Kim D, Paggi JM, Park C, Bennett C, Salzberg SL (2019) Graph-based genome alignment and genotyping with HISAT2 and HISAT-genotype. Nat Biotechnol 37:907–915. https://doi.org/10.1038/s41587-019-0201-4
Kosugi S, Ohashi Y (2002) DNA binding and dimerization specificity and potential targets for the TCP protein family. Plant J 30:337–348. https://doi.org/10.1046/j.1365-313X.2002.01294.x
Li M, Wei Q, Xiao Y, Peng F (2018) The effect of auxin and strigolactone on ATP/ADP isopentenyltransferase expression and the regulation of apical dominance in peach. Plant Cell Rep 37:1693–1705. https://doi.org/10.1007/s00299-018-2343-0
Li G, Tan M, Ma J, Cheng F, Li K, Liu X, Zhao C, Zhang D, Xing L, Ren X, Han M, An N (2021) Molecular mechanism of MdWUS2 MdTCP12 interaction in mediating cytokinin signaling to control axillary bud outgrowth. J Exp Bot 72:4822–4838. https://doi.org/10.1093/jxb/erab163
Liu Z, Yang J, Li S, Liu L, Qanmber G, Chen G, Duan Z, Zhao N, Wang G (2021) Systematic characterization of TCP gene family in four cotton species revealed that GhTCP62 regulates branching in *Arabidopsis*. Biology (Basel) 10:1104. https://doi.org/10.3390/biology10111104
Liu T, Dong L, Wang E, Liu S, Cheng Y, Zhao J, Xu S, Liang Z, Ma H, Nie B, Song B (2023) StHAB1, a negative regulatory factor in abscisic acid signaling, plays crucial roles in potato drought tolerance and shoot branching. J Exp Bot 74:6708–6721. https://doi.org/10.1093/jxb/erad292
Livak KJ, Schmittgen TD (2001) Analysis of relative gene expression data using real-time quantitative PCR and the 2(T)(−Delta Delta C) method. Methods 25:402–408. https://doi.org/10.1006/meth.2001.1262
Luo Z, Janssen BJ, Snowden KC (2021) The molecular and genetic regulation of shoot branching. Plant Physiol 187:1033–1044. https://doi.org/10.1093/plphys/kiab071
Lyu J, Huang L, Zhang S, Zhang Y, He W, Zeng P, Zeng Y, Huang G, Zhang J, Ning M, Bao Y, Zhao S, Fu Q, Wade LJ, Chen H, Wang W, Hu F (2020) Neo-functionalization of a Teosinte branched 1 homologue mediates adaptations of upland rice. Nat Commun 11:725. https://doi.org/10.1038/s41467-019-14264-1
Mansilla N, Fonouni-Farde C, Ariel F, Lucero L (2023) Differential chromatin binding preference is the result of the neo-functionalization of the TB1 clade of TCP transcription factors in grasses. New Phytol 237:2088–2103. https://doi.org/10.1111/nph.18664
Martin-Trillo M, Cubas P (2010) TCP genes: a family snapshot ten years later. Trends Plant Sci 15:31–39. https://doi.org/10.1016/j.tplants.2009.11.003
Maurya JP, Miskolczi PC, Mishra S, Singh RK, Bhalerao RP (2020) A genetic framework for regulation and seasonal adaptation of shoot architecture in hybrid aspen. Proc Natl Acad Sci USA 117:11523–11530. https://doi.org/10.1073/pnas.2004705117
Minakuchi K, Kameoka H, Yasuno N, Umehara M, Luo L, Kobayashi K, Hanada A, Ueno K, Asami T, Yamaguchi S, Kyozuka J (2010) FINE CULM1 (FC1) works downstream of strigolactones to inhibit the outgrowth of axillary buds in rice. Plant Cell Physiol 51:1127–1135. https://doi.org/10.1093/pcp/pcq083
Muhr M, Paulat M, Awwanah M, Brinkkötter M, Teichmann T (2018) CRISPR/Cas9-mediated knockout of Populus BRANCHED1 and BRANCHED2 orthologs reveals a major function in bud outgrowth control. Tree Physiol 38:1588–1597. https://doi.org/10.1093/treephys/tpy088
Müller D, Waldie T, Miyawaki K, To JPC, Melnyk CW, Kieber JJ, Kakimoto T, Leyser O (2015) Cytokinin is required for escape but not release from auxin mediated apical dominance. Plant J 82:874–886. https://doi.org/10.1111/tpj.12862

Nguyen TQ, Emery RJN (2017) Is ABA the earliest upstream inhibitor of apical dominance? J Exp Bot 68:881–884. https://doi.org/10.1093/jxb/erx028

Ni J, Gao C, Chen M, Pan B, Ye K, Xu Z (2015) Gibberellin promotes shoot branching in the perennial woody plant *Jatropha curcas*. Plant Cell Physiol 56:1655–1666. https://doi.org/10.1093/pcp/pcv089

Ni J, Zhao M, Chen M, Pan B, Tao Y, Xu Z (2017) Comparative transcriptome analysis of axillary buds in response to the shoot branching regulators gibberellin A3 and 6-benzyladenine in *Jatropha curcas*. Sci Rep 7:11417. https://doi.org/10.1038/s41598-017-11588-0

Pino LE, Lima JE, Vicente MH, de Sá AFL, Pérez-Alfocea F, Albacete A, Costa JL, Werner T, Schmülling T, Freschi L, Figueira A, Zsögön A, Peres LEP (2022) Increased branching independent of strigolactone in cytokinin oxidase 2-overexpressing tomato is mediated by reduced auxin transport. Mol Hortic 2:12. https://doi.org/10.1186/s43897-022-00032-1

Pruneda-Paz JL, Breton G, Para A, Kay SA (2009) A functional genomics approach reveals CHE as a component of the *Arabidopsis* circadian clock. Science 323:1481–1485. https://doi.org/10.1126/science.1167206

Qiu Y, Guan SC, Wen C, Li P, Gao Z, Chen X (2019) Auxin and cytokinin coordinate the dormancy and outgrowth of axillary bud in strawberry runner. BMC Plant Biol 19:528. https://doi.org/10.1186/s12870-019-2151-x

Rabot A, Henry C, Ben Baaziz K, Mortreau E, Azri W, Lothier J, Hamama L, Boummaza R, Leduc N, Pelleschi-Travier S, Le Gourrierec J, Sakr S (2012) Insight into the role of sugars in bud burst under light in the rose. Plant Cell Physiol 53:1068–1082. https://doi.org/10.1093/pcp/pcs051

Rameau C, Bertheloot J, Leduc N, Andrieu B, Foucher F, Sakr S (2015) Multiple pathways regulate shoot branching. Front Plant Sci 5:741. https://doi.org/10.3389/fpls.2014.00741

Salam BB, Barbier F, Danieli R, Teper-Bamnolker P, Ziv C, Spichal L, Aruchamy K, Shnaider Y, Leibman D, Shaya F, Carmeli-Weissberg M, Gal-On A, Jiang J, Ori N, Beveridge C, Eshel D (2021) Sucrose promotes stem branching through cytokinin. Plant Physiol 185:1708–1721. https://doi.org/10.1093/plphys/kiab003

Shen J, Zhang Y, Ge D, Wang Z, Song W, Gu R, Che G, Cheng Z, Liu R, Zhang X (2019) CsBRC1 inhibits axillary bud outgrowth by directly repressing the auxin efflux carrier CsPIN3 in cucumber. Proc Natl Acad Sci USA 116:17105–17114. https://doi.org/10.1073/pnas.1907968116

Shen J, Ge D, Song X, Xiao J, Liu X, Che G, Gu R, Wang Z, Cheng Z, Song W, Liu L, Chen J, Han L, Yan L, Liu R, Zhou Z, Zhang X (2021) Roles of CsBRC1-like in leaf and lateral branch development in cucumber. Plant Sci 302:110681. https://doi.org/10.1016/j.plantsci.2020.110681

Shimizu-Sato S, Tanaka M, Mori H (2009) Auxin-cytokinin interactions in the control of shoot branching. Plant Mol Biol 69:429-435. https://doi.org/10.1007/s11103-008-9416-3

Sparkes IA, Runions J, Kearns A, Hawes C (2006) Rapid, transient expression of fluorescent fusion proteins in tobacco plants and generation of stably transformed plants. Nat Protoc 1:2019–2025. https://doi.org/10.1038/nprot.2006.286

Steiner E, Yanai O, Efroni I, Ori N, Eshed Y, Weiss D (2012) Class I TCPs modulate cytokinin-induced branching and meristematic activity in tomato. Plant Signal Behav 7:807–810. https://doi.org/10.4161/psb.20606

Tahtiharju S, Rijpkema AS, Vetterli A, Albert VA, Teeri TH, Elomaa P (2012) Evolution and diversification of the CYC/TB1 gene family in *Asteraceae*-a comparative study in Gerbera (*Mutisieae*) and Sunflower (*Heliantheae*). Mol Biol Evol 29:1155–1166. https://doi.org/10.1093/molbev/msr283

Tan M, Li G, Chen X, Xing L, Ma J, Zhang D, Ge H, Han M, Sha G, An N (2019) Role of cytokinin, strigolactone, and auxin export on outgrowth of axillary buds in apple. Front Plant Sci. https://doi.org/10.3389/fpls.2019.00616

Tanaka M, Takei K, Kojima M, Sakakibara H, Mori H (2006) Auxin controls local cytokinin biosynthesis in the nodal stem in apical dominance. Plant J 45:1028–1036. https://doi.org/10.1111/j.1365-313X.2006.02656.x

Tu Z, Hao Z, Zhong W, Li H (2019) Identification of suitable reference genes for RT-qPCR assays in *Liriodendron chinense* (Hemsl.) Sarg. Forests 10:441–456. https://doi.org/10.3390/f10050441

Wagner GP, Kin K, Lynch VJ (2012) Measurement of mRNA abundance using RNA-seq data: RPKM measure is inconsistent among samples. Theory Biosci 131:281–285. https://doi.org/10.1007/s12064-012-0162-3

Waldie T, Leyser O (2018) Cytokinin targets auxin transport to promote shoot branching. Plant Physiol 177:803–818. https://doi.org/10.1104/pp.17.01691

Wang Z, Gerstein M, Snyder M (2009) RNA-Seq: a revolutionary tool for transcriptomics. Nat Rev Genet 10:57–63. https://doi.org/10.1038/nrg2484

Wang Y, Wang J, Shi B, Yu T, Qi J, Meyerowitz EM, Jiao Y (2014) The stem cell niche in leaf axils is established by auxin and cytokinin in *Arabidopsis*. Plant Cell 26:2055–2067. https://doi.org/10.1105/tpc.114.123083

Wang J, Tian C, Zhang C, Shi B, Cao X, Zhang T, Zhao Z, Wang J, Jiao Y (2017) Cytokinin signaling activates WUSCHEL expression during axillary meristem initiation. Plant Cell 29:1373–1387. https://doi.org/10.1105/tpc.16.00579

Wang M, Le Moigne MA, Bertheloot J, Crespel L, Perez-Garcia MD, Oge L, Demotes-Mainard S, Hamama L, Daviere JM, Sakr S (2019) BRANCHED1: a key hub of shoot branching. Front Plant Sci 10:76. https://doi.org/10.3389/fpls.2019.00076

Wei X, Yang J, Lei D, Feng H, Yang Z, Wen G, He Z, Zeng W, Zou J (2021) The SlTCP26 promoting lateral branches development in tomato. Plant Cell Rep 40:1115–1126. https://doi.org/10.1007/s00299-021-02680-x

Wu Y, Zhang J, Li C, Deng X, Wang T, Dong L (2023) Genome-wide analysis of TCP transcription factor family in sunflower and identification of HaTCP1 involved in the regulation of shoot branching. BMC Plant Biol 23:222. https://doi.org/10.1186/s12870-023-04211-0

Xia X, Dong H, Yin Y, Song X, Gu X, Sang K, Zhou J, Shi K, Zhou Y, Foyer CH, Yu J (2021) Brassinosteroid signaling integrates multiple pathways to release apical dominance in tomato. Proc Natl Acad Sci USA 118:e2004384118. https://doi.org/10.1073/pnas.2004384118

Xiang C, Wang Z (2012) A new scientific name of hybrid *Liriodendron—L. sino-americanum*. J Nanjing For Univ 36:1–2

Xu T, Liu X, Wang R, Dong X, Guan X, Wang Y, Jiang Y, Shi Z, Qi M, Li T (2016) SlARF2a plays a negative role in mediating axillary shoot formation. Sci Rep 6:33728. https://doi.org/10.1038/srep33728

Yamada H, Suzuki T, Terada K, Takei K, Ishikawa K, Miwa K, Yamashino T, Mizuno T (2001) The *Arabidopsis* AHK4 histidine kinase is a cytokinin-binding receptor that transduces cytokinin signals across the membrane. Plant Cell Physiol 42:1017–1023. https://doi.org/10.1093/pcp/pce127

Yokoyama A, Yamashino T, Amano YI, Tajima Y, Imamura A, Sakakibara H, Mizuno T (2007) Type-B ARR transcription factors, ARR10 and ARR12, are implicated in cytokinin-mediated regulation of protoxylem differentiation in roots of *Arabidopsis thaliana*. Plant Cell Physiol 48:84–96. https://doi.org/10.1093/pcp/pcl040

Young NF, Ferguson BJ, Antoniadi I, Bennett MH, Beveridge CA, Turnbull CGN (2014) Conditional auxin response and differential

cytokinin profiles in shoot branching mutants. Plant Physiol 165:1723–1736. https://doi.org/10.1104/pp.114.239996

Zhang Q, Wang J, Wang L, Wang J, Wang Q, Yu P, Bai M, Fan M (2020) Gibberellin repression of axillary bud formation in *Arabidopsis* by modulation of DELLA-SPL9 complex activity. J Integr Plant Biol 62:421–432. https://doi.org/10.1111/jipb.12818

Zhang L, Fang W, Chen F, Song A (2022) The role of transcription factors in the regulation of plant shoot branching. Plants (Basel) 11:1997. https://doi.org/10.3390/plants11151997

Zhao M, Peng X, Chen N, Shen S (2020) Genome wide identification of the TCP gene family in *Broussonetia papyrifera* and functional analysis of BpTCP8, 14 and 19 in shoot branching. Plants (Basel) 9:1301. https://doi.org/10.3390/plants9101301

Zhao Q, Chen H, Zhang D, Ma J (2023) Ectopic expression of the apple cytokinin response regulator MdRR9 gene in tomatoes promotes shoot branching. Sci Hortic. https://doi.org/10.1016/j.scienta.2023.112228

Zhou H, Hwarari D, Ma H, Xu H, Yang L, Luo Y (2022) Genomic survey of TCP transcription factors in plants: phylogenomics, evolution and their biology. Front Genet 13:1060546. https://doi.org/10.3389/fgene.2022.1060546

Publisher's Note Springer Nature remains neutral with regard to jurisdictional claims in published maps and institutional affiliations.

Springer Nature or its licensor (e.g. a society or other partner) holds exclusive rights to this article under a publishing agreement with the author(s) or other rightsholder(s); author self-archiving of the accepted manuscript version of this article is solely governed by the terms of such publishing agreement and applicable law.